1968

A study of $BiFeO_3$ and the Hall effect in $BiFeO_3$ and CdS

Fred Hoerger Taylor

Department:

A STUDY OF $BiFeO_3$ AND THE HALL EFFECT IN $BiFeO_3$ AND CdS

BY

FRED HOERGER TAYLOR

AN

ABSTRACT

submitted to the faculty of

THE UNIVERSITY OF MISSOURI - ROLLA

in partial fulfillment of the requirements for the

Degree of

MASTER OF SCIENCE IN PHYSICS

Rolla, Missouri

1968

Approved by

Robert Iverson (advisor) W. J. James

Otto L. Hill

ABSTRACT

Pure samples of $BiFeO_3$ were heat treated in oxygen and nitrogen atmospheres in an attempt to reduce the conductivity of the samples. Dielectric constant and dissipation factor measurements, as a function of frequency, were made to determine whether the samples had been altered.

A special high temperature Hall effect apparatus was constructed. Using this apparatus an upper limit for the Hall mobility in $BiFeO_3$ was established. The apparatus was also used for room temperature measurements on Ga-doped CdS samples. Resistivity measurements to be used with the Hall effect results were made on both the $BiFeO_3$ and the CdS samples.

Hot-Point Probe (thermoelectric) measurements on $BiFeO_3$ indicated p-type conduction, and the Hall effect results established n-type conduction for the CdS samples.

ACKNOWLEDGEMENTS

The author wishes to express his appreciation to Dr. R. Gerson, Professor of Physics, for the suggestion of the problem and his guidance throughout this investigation. The author would also like to thank J. Canner of the Physics Department for his help in hot pressing the samples used, and Mrs. Roberta Lamar of the Materials Research Center for preparing the samples.

The author would like to acknowledge the financial support of the Atomic Energy Commission (Project AT(11-1) 1368) during this investigation.

The encouragement during preparation as well as the typing of the manuscript by the author's wife Kathleen is appreciated.

TABLE OF CONTENTS

LIST OF TABLES

LIST OF FIGURES

I. INTRODUCTION

In recent years there has been an increased amount of scientific activity in the area of ferroelectricity. This work can be divided into two main areas of study. These are the investigation, from a structural point of view, of the properties of ferroelectrics and suspect ferroelectrics and more recent attempts to give a more general theoretical basis to the phenomenon of ferroelectricity. Of the four major divisions of ferroelectrics those having the perovskite structure have been the subject of a major portion of this increased scientific activity, because of their comparatively simple crystal structure. A new perovskite compound with ferroelectric or antiferroelectric properties has been reported recently in the literature. This new compound is bismuth ferrate ($BiFeO_3$).

Dielectric measurements in the past have been made of solid solutions of $BiFeO_3$ with other compounds of perovskite structure. Extrapolation techniques were then used to infer the properties of pure $BiFeO_3$. Recently published high frequency dielectric results seem to indicate that pure $BiFeO_3$ is ferroelectric, but at this time antiferroelectricity has not been completely eliminated as a possibility. Dielectric measurements have been hard to obtain because of the high conductivity of ceramic samples at a temperature near the Curie temperature. The unavailability of single crystals has also hampered research on pure $BiFeO_3$.

The purpose of this work was to try to alter the conductivity of pure $BiFeO_3$. The conductivity in the pure $BiFeO_3$ samples has been attributed to

the presence of the Fe^{++} ion in the lattice. This ion would tend to increase the electronic hopping conductivity between iron ions. In this work we tried to reoxidize the pure $BiFeO_3$ at high temperatures, thus reducing the conductivity. Samples were also heat treated in a reducing (nitrogen) atmosphere.

The heat treated material was then hot pressed into ceramic samples for low frequency dielectric measurements and Hall effect measurements. It was possible to change the conductivity of the ceramic samples somewhat. Attempts to measure the Hall effect were unsuccessful, however.

Hall effect measurements were made on two samples of Ga-doped CdS for other researchers working in the Physics Department. These measurements served as a check of our experimental apparatus.

II. REVIEW OF LITERATURE

A. Definition of Ferroelectricity

In 1921 the phenomenon of ferroelectricity was discovered by Valasek.[1] While working with Rochelle salt he found that it exhibited what he called a dielectric hysteresis analogous to magnetic hysteresis. The existence in a crystal of a dielectric hysteresis loop implies that the crystal possesses a spontaneous polarization, which is a polarization that persists after the field is removed. Thus, in analogy to ferromagnetism, this new phenomenon became known as ferroelectricity. The spontaneous polarization in a ferromagnet corresponds to intrinsic magnetization. While a magnetic moment can be detected and measured by its external field, electric polarization can be only similarly detected if the crystal retains charge on its surface. However, such a charge becomes neutralized by the collection on the crystal surface of free charges and by conduction within the crystal. By applying an electric field opposite to the direction of polarization the polarization can be reversed, if the field is larger than the coercive field. If not, the polarization remains unobservable. The spontaneous polarization is a very important property of ferroelectricity. Megaw[2] has defined ferroelectricity as follows, "A ferroelectric is a crystal possessing reversible polarization, as shown by a dielectric hysteresis loop". Kittel,[3] Burfoot,[4] Jona and Shirane,[5] and Fatuzzo and Merz[6] have all defined ferroelectricity in a similar manner.

Since all ferroelectrics are crystalline and solids,[7] it would be desirable to define ferroelectricity from a crystal classification point of view. Any

crystal may be classified, according to the symmetry which it possesses, into one of thirty-two crystal classes (point groups).[8] Eleven of these point groups are characterized by a center of symmetry and thus may possess no polar properties. The remaining twenty-one point groups have no center of symmetry (non-centrosymmetric) and may possess one or more polar axes and thus show vectorial or tensorial properties. Of the twenty-one non-centrosymmentric point groups, twenty may exhibit piezoelectricity, but group 432 may not exhibit piezoelectricity. Burfoot[9] has defined a piezoelectric as a crystal having the property of acquiring electric polarization under external mechanical stresses, and conversely the property of changing size and shape when subjected to external electric fields. There is a subgroup, of ten groups, of these twenty piezoelectric groups which have a unique polar axis. Crystals in these classes are called pyroelectric groups which have a unique polar axis. Crystals in these classes are called pyroelectric and show a spontaneous polarization. As mentioned before the spontaneous polarization generally cannot be detected by charges on the surface because they have been compensated by internal and external conduction, and by twinning. Ferroelectric crystals belong to the pyroelectric family, but have the added restrictions that it must be possible to reverse the direction of spontaneous polarization by application of an electric field. Thus a necessary condition for ferroelectricity is that it belongs to one of the ten pyroelectric classes, but this is not sufficient, as reversibility of polarization must also occur. The existence of a unique polar axis in a crystal' s point group symmetry may be established by means of x-ray analysis, but only dielectric measurements can establish reversibility.

B. Classification of Ferroelectrics

The classification of ferroelectric crystals has been attempted by several authors with a limited degree of success. Jona and Shirane[10] have listed the following four possible methods of classification, but state that a consistent classification of all ferroelectric crystals at this time is hardly possible:

1. Crystal chemical classification dividing ferroelectrics into two groups. Hydrogen bonded crystals such as KH_2PO_4, Rochelle salt, and triglycerine sulfate form group one, while the double oxides such as $BaTiO_3$, $KNbO_3$, $Cd_2Nb_2O_7$, $PbNb_2O_2$ form group two.
2. Classification according to the number of allowed directions of spontaneous polarization. There are two groups in this classification also: those having only one allowed direction of polarization, and those having more than one direction of polarization.
3. Classification according to the existence or lack of a central symmetry in the point group of the non polar phase.
4. Classification according to the nature of the phase change occurring at the Curie point. Group one would contain those ferroelectrics which undergo an order-disorder type of transition, while a second group contains those

ferroelectrics that undergo a transition of the displacive type, such as $BaTiO_3$ and other double oxides.

A classification different from any of those mentioned above has been made by Kittel[11] and Megaw.[12] The classification is as follows:

1. Rochelle salt ($NaKC_4H_4O_6 \cdot 4H_2O$). This group includes Rochelle salt and its deuterium-substituted analogue. Solid solutions in which there is a small amount of isomorphous replacement of K and Na by other ions are also included.
2. Potassium hydrogen phosphate (KH_2PO_4). This group comprises the phosphates and arsenates of all the alkali metals K, Rb, Cs, and their deuterium-substituted analogues. These crystals have a hydrogen bond in which the motion of the protons is specifically connected with ferroelectricity.
3. Barium titanate ($BaTiO_3$). This group consists of ionic crystals with the perovskite and ilmenite structure, or crystals with a structure very close to these structures. Members of this group include PbTiO, $KNbO_3$, $NaNbO_3$, $KTaO_3$, WO_3, $LiNbO_3$ and many solid solutions of materials having this structure.

4. Miscellaneous. This group consists of guanidine compounds and other miscellaneous compounds. The mechanism of ferroelectricity in these compounds is not well understood.

C. Properties of Ferroelectric Crystals

Several of the properties of ferroelectric crystals have already been mentioned or implied in defining the phenomenon of ferroelectricity. Some or all of the following properties, as summarized by Megaw,[13] are possessed by most ferroelectrics:

1. "They possess a dielectric hysteresis loop, indicating reversible spontaneous polarization.
2. They show disappearance of hysteresis at a certain temperature, the Curie temperature.
3. They have a domain structure which may be visible in polarized light.
4. They have a high dielectric constant, rising to a peak at the Curie point.
5. The falling off of their dielectric constants above the Curie point follows a Curie-Weiss law.
6. They possess a pseudosymmetric structure.
7. Their symmetry places them in a polar class.
8. They have a transition at the Curie point to a form of higher symmetry.

9. The Curie point is raised (or a lower Curie point lowered) by the application of a biasing field.

10. There is a sudden appearance of surface charges at the transition."

As previously stated property 1 may be used to define ferroelectricity, and it is then a necessary condition for the existence of ferroelectricity. Figure 1 shows an example of a dielectric hysteresis loop for a typical ferroelectric material. Properties 6 and 7 are necessary conditions for the existence of ferroelectricity. The pseudosymmetric structure mentioned above is associated with the ferroelectric or antiferroelectric state which is present below the Curie point. Above the Curie point there is a transition to a form of higher symmetry, sometimes called the paraelectric state in analogy to paramagnetic states in magnetic materials.

The Curie-Weiss law mentioned in property 5 is of the form,

$$\epsilon = \frac{C}{T - T_c} \qquad (1)$$

where ϵ is the dielectric constant, C is the Curie constant, T is the crystal temperature, and T_c is the Curie temperature, which usually coincides or is very close to the transition temperature. It should be emphasized that Equation 1 refers only to the high temperature side of any existent Curie point and does not guarantee the existence of ferroelectricity below the Curie point. The behavior of the dielectric constant in the region of the Curie point is illustrated in Figure 2 for a ferroelectric and antiferroelectric material. The increase in

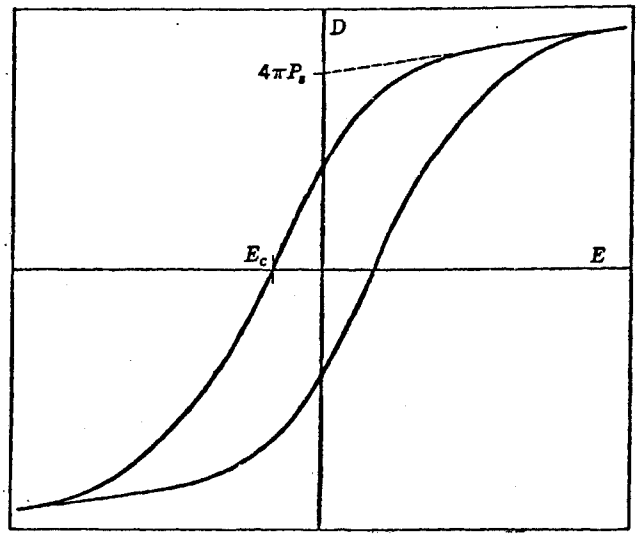

Fig. 8.3. Hysteresis loop in ferroelectric specimen, showing spontaneous polarization P_s and coercive field E_c. In barium titanate the value of $4\pi P_s$ may be of the order of 3×10^8 v/cm, and E_c of the order of 10^3 v/cm.

Figure 1. Hysteresis loop for ferroelectric material(3)

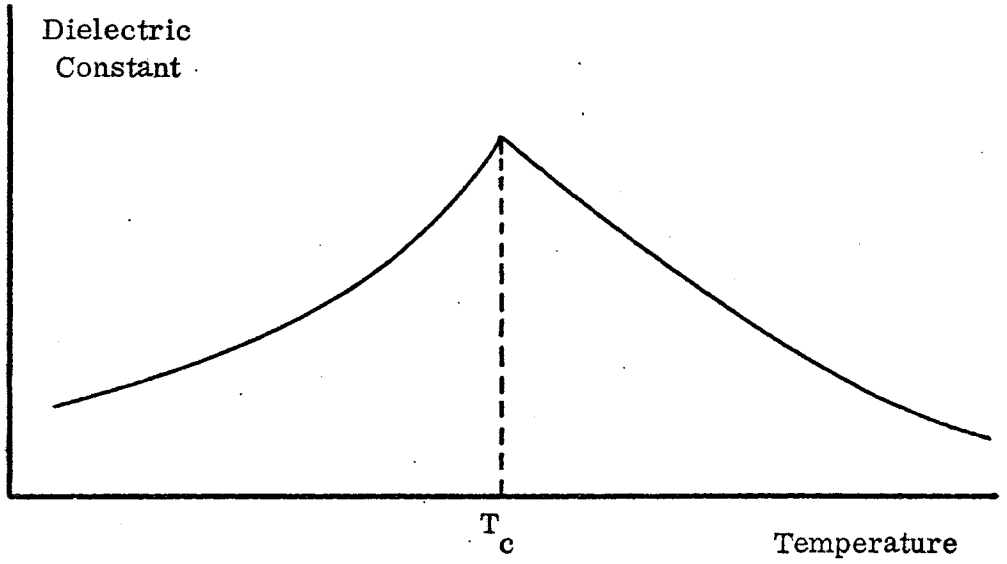

FERROELECTRIC BEHAVIOR

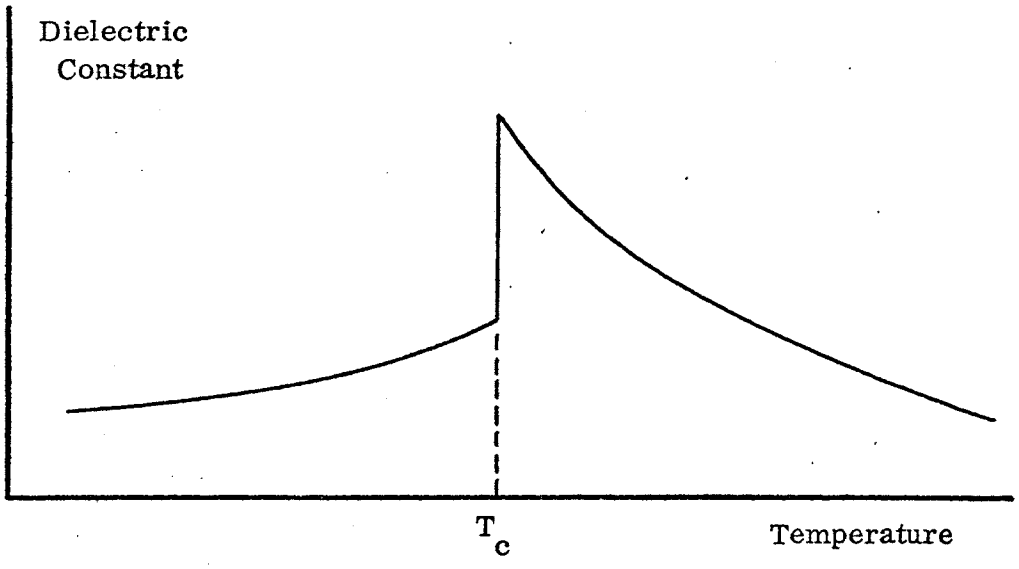

ANTIFERROELECTRIC BEHAVIOR

Figure 2. Dielectric constant as a function of temperature for ferroelectric and antiferroelectric materials

the dielectric constant for the ferroelectric material is a result of the increase in polarization of the material. This is referred to as the polarization catastrophe and it can be shown[14] the dielectric constant becomes very large for finite polarization. The antiferroelectric material also has an anomaly in the dielectric constant at the Curie point although it is generally lower in an antiferroelectric than in a ferroelectric material.

Figure 3 shows actual experimental results for ferroelectric $BaTiO_3$ and antiferroelectric $PbZrO_3$ as given in Kittel.[15]

Some of the differences between ferroelectrics and antiferroelectrics and some of the properties of antiferroelectrics have already been mentioned. The existence of materials having no spontaneous polarization because individual parts of the structure have polarizations in opposite senses was predicted by Kittel[16] in 1951. The first of these, called antiferroelectrics, was lead zirconate ($PbZrO_3$). Megaw[17] defines antiferroelectricity as follows: "An antiferroelectric is a substance of non-polar symmetry, showing no dielectric hysteresis, which has a pseudosymmetric transition to a high symmetry form accompanied by a sharp anomaly in the dielectric constant." It is not certain whether any materials exist which completely satisfy this definition.

D. Perovskite Structure

A large number of compounds,[18][19][20] of the general formula ABX_3, possess the structure of the perovskite family. Many, but not all, the members of the perovskite family are ferroelectric or antiferroelectric in nature. The

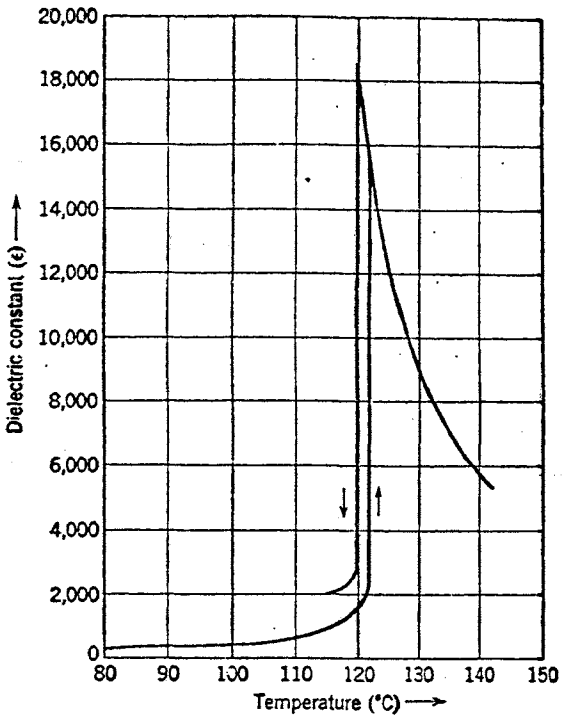

Fig. 8.8. Dielectric constant of barium titanate vs. temperature. [After M. E. Drougard and D. R. Young, Phys. Rev. 95, 1152 (1954).]

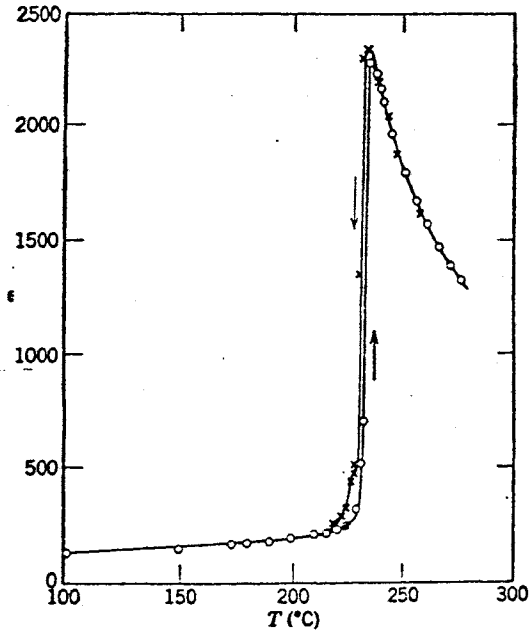

Fig. 8.19. Dielectric constant of lead zirconate at varying temperatures. (After Shirane, Sawaguchi, and Takagi.)

Figure 3. Dielectric constant as a function of temperature for ferroelectric $BaTiO_3$ and antiferroelectric $PbZrO_3$ [3]

group gets its name from the naturally occurring mineral perovskite ($CaTiO_3$). Of the four groups of ferroelectric crystals the perovskite family has been the target of an extensive amount of past and present research. Much of the present work has been in the synthesis and subsequent investigation, for ferroelectricity, of new compounds and solid solutions.

In the general chemical formula the A cation is a relatively large ion having coordination 12, while the B cation is smaller and has 6 coordination. The X ion is generally oxygen, but, there are known compounds where this ion is fluorine. The double oxides are ferroelectric and antiferroelectric, while the known double fluorides are not reported to be ferroelectric in nature.

The perovskite crystal structure is cubic with A ions at the corners, oxygen ions at the face centers, and B ions at the body center. An alternate interpretation is a three dimensional network of BO_6 octahedra, where each B ion is at the center of six oxygen ions arranged at the corners of a regular octahedron. One of these octahedra occupies each corner of a cubic three dimensional network enclosing large holes which contain the large A cation. Both of these interpretations are shown in Figure 4. The structure just discussed is the ideal cubic perovskite structure, however, and the perovskite family includes three other pseudosymmetric structures. Megaw[21] makes the following classification of oxides with the chemical formula ABO_3:

1. Cubic perovskite. A large number of compounds possesses the ideal cubic structure with cell edge a_o about 4 Å, and cell contents one formula unit. For many of these, no

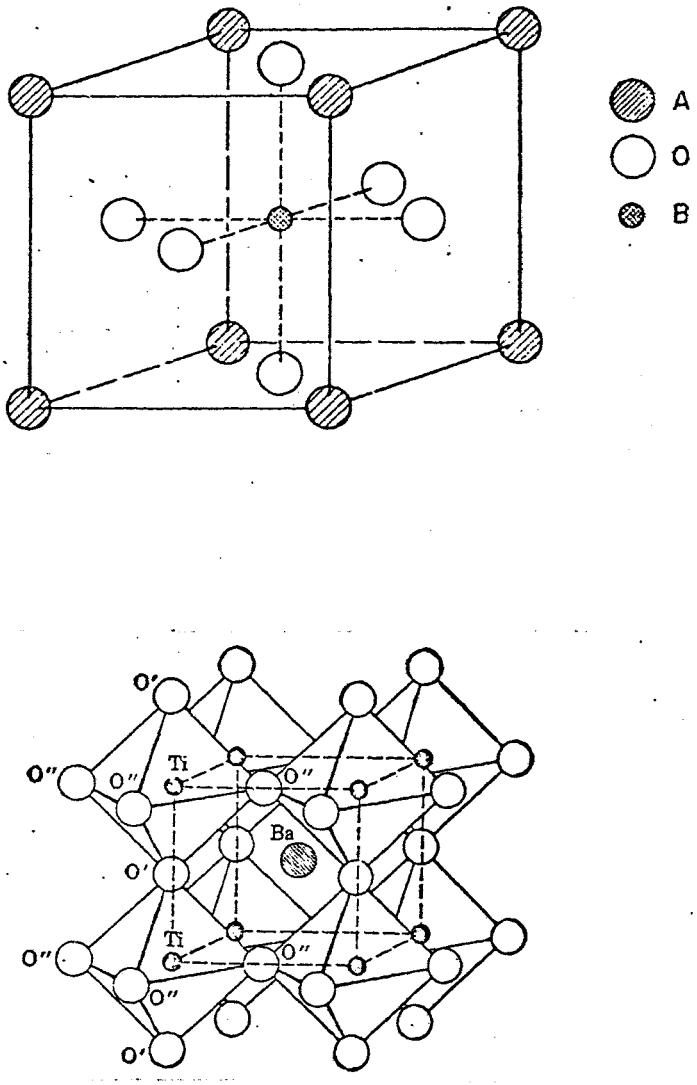

Figure 4. The perovskite structure[3][5]

other structure is known, and they are not ferroelectric. The crystalline tolerance factor, t, (defined below) lies between 1.05 and 0.90.

2. Distorted small cell perovskite. A few substances for which t is nearly unity have one or more low temperature forms with a distorted small cell. Therefore, they are no longer cubic, but if referred to the original axis, the cell edges are still approximately 4 Å. Whatever the choice of axis, they still have only one formula-unit per lattice point. Examples of this class are: $BaTiO_3$, $PbTiO_3$, and $KNbO_3$. All known structures are ferroelectric and they have a transition to ideal cubic structures when ferroelectricity disappears.

3. Distorted multiple-cell perovskite. Many substances possess a distorted structure in which adjacent units of 4 Å edges are not perfectly identical, though nearly so. The true cell is made up of a number of these sub-cells. Thus, if it is referred to the original axis, its edges are all nearly multiples of $a_o \cong 4$Å; but it may be more convenient to use axes on which they are nearly multiples of $\sqrt{2}a_o$.

4. Other types, including ilmenite structures. These occur when the tolerance factor t falls below a limit which is about 0.75 for compounds where A has valency 1, and which increases with the valency of A.

If the ions in the cubic close packing arrangement of Figure 4 (top) are considered as hard spheres, the sum of an A ion diameter and an oxygen diameter form a face diagonal, while the sum of the B ion diameter and an oxygen diameter form a cube edge. Thus, for perfect packing the following relations must hold:

$$R_a + R_o = \sqrt{2}\,(R_b + R_o) \qquad (2)$$

where,

R_a = radius of A ion.

R_b = radius of B ion.

R_o = radius of 0 ion.

Because of the large number of perovskite compounds known to exist it is necessary to introduce a tolerance factor which is indicative of the tolerance to fit for that particular compound. Formula 2 thus becomes,

$$R_a + R_o = t\sqrt{2}\,(R_b + R_o) \qquad (3)$$

where t is the tolerance factor. Goldschmidt[22] concluded and Keith and Roy[23] confirmed that the perovskite structure may be expected for ABO_3 compounds with a tolerance factor between 0.77 and 0.99. Later evidence shows that perovskite structure dominates when t is between 0.9 and 1.1, while the ilmenite structures occur for $t < 0.8$.

Goldschmidt[24] established a criteria for stability of ABX_3 compounds, which was later restated by Megaw[25] as follows: "An ion has a radius which does not vary by more than a few percent in the different structures in which the ion occurs. The sum of two such radii make up the observed cation-anion distance. When a cation and the surrounding anions are given their correct radii, all the anions must touch the cation. In other words, the cation must not "rattle" in the holes between the anions. The cation can only be surrounded by the number of anions which make contact with it."

For electrical neutrality the valencies of the A and B cations must sum up to 6, to balance the three oxygen anions in each formula unit. This leads to the following three types of double oxide; A(+1) B(+5) O_3, A(+2) B(+4) O_3, and A(+3) B(+3) O_3. All three of the above have been reported and shown to have the perovskite structure. Ferroelectrics, until recently, have tended to satisfy the criterion set by Matthias:[26] The B ions in the ferroelectric shall possess a rare gas electronic configuration. $BiFeO_3$, the subject of this work can be shown not to satisfy the ideal gas configuration because of the incomplete d shell of the Fe^{3+} ion. It has been stated[27][28] that the electronic structure of Fe^{3+} is close to the Matthias criterion.

E. Bismuth Ferrate

In spite of an extensive amount of investigation, by several different groups of researchers, the exact nature of $BiFeO_3$ still remains unknown.

The dielectric work has been extremely hampered because of the conductivity of a ceramic sample of pure $BiFeO_3$. The structural investigations

have, until recently, been hampered by the lack of single phase material, and by the fact that the Fe ion has a tendency to assume multiple valencies, thus upsetting the stoichiometry of the pure $BiFeO_3$ or its solid solutions. The structural work has also been slowed by the lack of single crystals of suitable size.

Polycrystalline samples of $BiFeO_3$ were reported in the literature in 1960 by Filipev et al.[29] and Venevtsev et al.[30] X-ray diffraction yielded a perovskite structure having rhombohedral distortion and the following room temperature unit cell parameters: $a_o = 3.957$ Å, $\alpha = 89^o28'$. On the basis of these early x-ray diffraction results the following space groups were proposed: $R\bar{3}$, R3, R32, $R\bar{3}m$. Zaslavskii and Tutov[31] concluded that the structure should be $R\bar{3}m$, but this result conflicts with the belief that $BiFeO_3$ is a ferroelectric, since the space group $R\bar{3}m$ does not allow ferroelectricity. Tomashpol'skii et al.,[32] in 1964, made an electron diffraction study of $BiFeO_3$ and concluded that there was one formula in the unit cell. They gave $BiFeO_3$ the space group R3m, in contradiction of the result mentioned above. The space group R3m does allow ferroelectricity.

High temperature x-ray analysis by Fedulov et al.[33] indicated that the transition temperature, if existent, was above the melting point for pure $BiFeO_3$. Another x-ray study by Fedulov et al.[34] on the binary system $BiFeO-PbTiO_3$ established, by extrapolation, a Curie temperature for pure $BiFeO_3$ of 850^oC.

These early x-ray and electron diffraction studies were only an

approximation, because the scatting powers of the Bi and Fe ion for x-rays completely masks the contributions of the oxygen ions. In 1964 Kiselev et al.[35] made a neutron diffraction study of pure $BiFeO_3$. He assumed the low symmetry space group R3 as a first approximation and then, using a least squares analysis, was able to refine the structure to the R3m symmetry. This is the same result that Tomashpol'skii had arrived at in his electron diffraction work.

Additional high resolution neutron diffraction work by Plakhtii et al.,[36] in 1964, on polycrystalline $BiFeO_3$ at room and high temperature, indicated that all previous structural analyses had been incorrect. Superstructure peaks not attributable to a simple unit cell were observed. Plakhtii suggested a double unit cell similar to $LaAlO_3$ for $BiFeO_3$. It was also suggested that these results were indicative of antiferroelectricity in pure $BiFeO_3$.

Roginskaya et al.[37] suggested that the superstructure lines in the neutron diffraction patterns were due to the impurity phase $B_2O_3 \cdot 2Fe_2O_3$. This work consisted of x-ray and electron diffraction analysis on a single crystal.

Achenbach[38] also performed neutron diffraction work on pure $BiFeO_3$. He was able to prepare high purity $BiFeO_3$ using a technique slightly different from that being used by most researchers working with $BiFeO_3$. In this high purity material superstructure lines were still present in neutron diffraction patterns, and thus it was concluded that the unit cell probably contained two formula units.

The magnetic nature of $BiFeO_3$ was suspected because of the $Fe^{3+} - O^{2-} - Fe^{3+}$ chains of ions present in the structure. Smolenskii et al.[39] confirmed

the expected antiferromagnetic behavior of $BiFeO_3$, and he found a Neel temperature of 370°C. However, he also found that magnetic susceptibility displayed a sharp peak at the Neel temperature, a characteristic of weak ferromagnetism. There was no observed spontaneous magnetic moment, and thus the possibility of the existence of weak ferromagnetism is still in question. Yudin[40][41] also reported the magnetic susceptibility exhibits a sharp peak at the Neel temperature, but again there was no spontaneous magnetic moment observed up to extremely high fields. Neutron diffraction studies by Kiselev[42][35] and Plakhtii[36] also show G type antiferromagnetic ordering in $BiFeO_3$. Mossbauer[43] and neutron diffraction studies[38] at the University of Missouri-Rolla have also confirmed the antiferromagnetic nature of $BiFeO_3$. In a recent work Latham[28] investigated the magnetic susceptibility and spontaneous magnetic moment of polycrystalline solid solutions of $BiFeO_3$ with $PbTiO_3$, $PbZO_3$ and (50% $PbZrO_3$ · 50% Pb TiO_3). He found a sharp peak in the susceptibility at the Neel temperature but no spontaneous magnetic moment. However, the solid solutions possessed a spontaneous magnetic moment throughout the multiple cell rhombohedral region. He suggested that this could be due to a small amount of atomic ordering rather than to weak ferromagnetism.

There is as much disagreement concerning the electrical nature of $BiFeO_3$ as there is about its structural and magnetic properties. Krainik et al.[44] support antiferroelectricity because of the low dielectric constant and the behavior of the relative linear expansion with increasing temperature. There is some question as to why these results were interpreted to mean

antiferroelectricity. These results are also subject to question because of the high conductivity of the samples. In his work with solid solutions [45] containing $BiFeO_3$ as one component he also concludes that pure $BiFeO_3$ is antiferroelectric. Smolenskii et al. [46] also conclude that $BiFeO_3$ is antiferroelectric, because pyroelectricity is forbidden for space group suggested for $BiFeO_3$ which also supports weak ferromagnetism. Roginskaya et al. [37] concluded from work on pure $BiFeO_3$ and solid solutions in the $BiFeO_3$ - $PbFe_{1/2}Nb_{1/2}O_3$ system that pure $BiFeO_3$ was ferroelectric. He also carried out an analysis of much of the previously published literature and gave the following reasons for concluding ferroelectricity:

1. "The presence of a continuous series of solid solutions in the $PbTiO_3$ - $BiFeO_3$ system and the increase in the Curie temperature of this system practically up to pure $BiFeO_3$.
2. The presence of maxima in the temperature dependence of the dielectric permittivity ϵ in some solid solutions based on $BiFeO_3$ (for example, in the system $BiFeO_3$ - $PbFe_{1/2}Nb_{1/2}O_3$).
3. Structure data on the noncentrosymmetric space group of $BiFeO_3$ and the lack of atomic superstructure; the rhombohedral cell distortion ($\alpha_{Rh} < 90^{o}$) typical of ferroelectrics.

4. Data on the resonance absorption of gamma quanta in $BiFeO_3$ indicating the absence of structurally non-equivalent positions of the iron atoms (which should occur in the case of antiferroelectricity).
5. The frequency dispersion of the dielectric permittivity ϵ and the maximum of the dielectric losses in the dispersion region which as a rule does not appear in antiferroelectrics."

One final point that should be mentioned is the possibility of electric and magnetic interactions. Roginskaya et al.[37] and Tomashpol' skii et al.[47] have reported changes in the unit cell parameters as well as anomalies in the dielectric constant at the Neel temperature. Krainik et al.[44] discounted this because of a phase transition occurring in $BiFeO_3$ near the Neel temperature. Latham[28] suggested that this transition may be the result of an electric and magnetic interaction, but he was unable to find any evidence of an interaction in his work.

In summary $BiFeO_3$ is an antiferromagnet, possibly possessing weak ferromagnetism, with a multiple unit cell. It is probably a ferroelectric material also, but not one possessing the smallest possible unit cell.

F. Cadmium Sulfide

The cadmium sulfide samples used in the Hall effect measurements were Ga-doped single crystals grown by the Electronic Research Division, Clevite Corporation. The two bar shaped samples were known to have approximately

the following properties: Hall mobility, 10^2 cm^2/volt sec; carrier concentration, 10^{18} - 10^{19} carriers/cc; and resistivity, 10^{-2} ohm cm.

The nature of the contact made by various materials has been investigated.[48][49] It was found that indium and gallium produce ohmic noise free contacts to cadium sulfide crystals. Contacts of Au, Ag, Cu, and Pt to CdS are generally rectifying, and of high resistence. A good ohmic contact is obtained by using In or Ga with a simple pressure contact to the crystal, and diffusing a small amount of the In or Ga into the surface of the crystal will also produce a good ohmic contact.

G. Conductivity and the Hall Effect

Before beginning the discussion of the theoretical and experimental aspects of the Hall effect, a brief summary of the evolution of conduction theory will be given. The early theory of the electrical properties of solids postulated the presence, in conducting solids, of a gas of free electrons behaving similar to an ordinary gas. In the free electron model the valence electrons, called conduction electrons, of the constituent atoms are able to move freely within the volume of the solid. It is also assumed that the interaction of the conduction electrons with the ion cores can be neglected. This theory is quite successful in the derivation of the form of Ohm's law which relates the electric current with the electric field, and the derivation of the relation between the electrical conductivity and the thermal conductivity.

There were, however, several very important results that this theory failed to predict or explain. By analogy tc an ideal gas it was expected that free

electrons would make a large contribution to the specific heat, but in fact the specific heats of conductors and insulators are very similar. The second difficulty was that the Bohr-Sommerfeld model of the atom predicted many electrons surrounding the nucleus, while the Hall effect measurements showed that only one electron per atom was concerned with the conduction process. The third and last difficulty was one that Hall effect measurements were quite instrumental in revealing, and this was the existence of positively charged carriers.

The first of these difficulties was taken care of by replacing Maxwell-Boltzmann statistics with Fermi-Dirac statistics. This modified free electron gas theory was able to predict the observed specific heat. The second and third difficulty were eliminated by the application of the principles of Quantum Mechanics and the Pauli exclusion principle. These considerations lead to what is now known as the band theory of solids. The band theory arises from consideration of the Bragg reflections undergone within a crystal because of the wave nature of an electron. These considerations lead to the existence of an energy gap in the distribution in energy of the states of the conduction electrons. These energy gaps appear because of the periodic nature of the crystal lattice.

The band theory explains why solids may be insulators, conductors, or semiconductors. If all of the energy levels below the forbidden energy band are filled, and all above are empty, the material will be an insulator. In a conductor the band just below the forbidden band is only partially filled and can contribute electrons to the conduction process. The width of these bands is

also of great importance. Any further consideration of the conduction process is beyond the scope of these introductory remarks and is covered in Kittel.[50]

The Hall effect was an investigatory tool of great importance in the development of these conduction theories. The Hall effect was discovered in 1879 by E. H. Hall[51] during an investigation of the nature of the force acting on a conductor carrying a current in a magnetic field. When a conducting crystal is placed in a magnetic field perpendicular to the direction of current flow there develops voltage across the sample which is perpendicular to both the current direction and the direction of the magnetic field. The voltage is called the Hall voltage.

The following discussion of the Hall effect[52][53][54] is referred to Figure 5 which shows the usual arrangement of samples and sample shapes for a Hall effect measurement. Assume that the sample has been doped with donor impurities, making the conductivity n-type (electronic). The bar has an electric field of strength E_x applied in the x direction and a magnetic field of strength B_z applied in the z direction.

The carrier velocity in the x direction due to the electric field E_x is given by:

$$\bar{v}_n = -\mu_n \bar{E}_x \tag{4}$$

where,

μ_n is the electron mobility in meters 2/volt-second

$\bar{v}_n$ is the drift velocity in meters/second

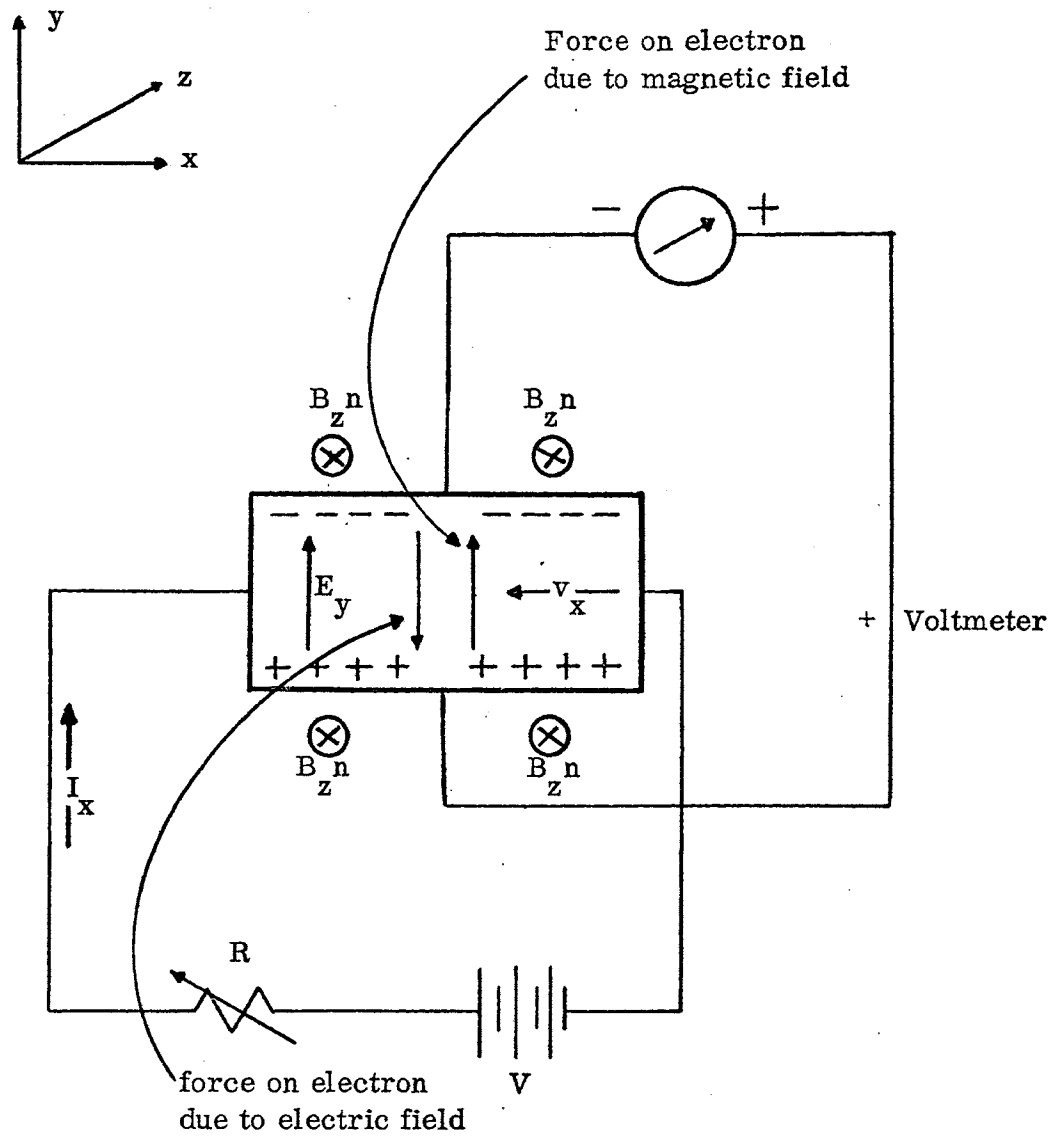

Figure 5. The Hall effect

The drift velocity $\bar{v}_n$ is perpendicular to the magnetic field, which gives rise to a Lorentz force on the carriers in the y direction given by:

$$F_y = -e\bar{v}_n \times \bar{B} \tag{5}$$

where the units for B are webers/meter^2. The minus signs in Equations (4) and (5) occur because we are considering negative carriers. Expanding the cross product in Equation (5) gives

$$F_y = ev_n B_z \tag{6}$$

for the Lorentz force on the carrier.

Under the influence of the Lorentz force electrons in the bar are accelerated upward, leaving an unneutralized layer of bound positive charges on the bottom of the bar. The net negative and net positive charges on the upper and lower surfaces of the sample establishes an electric field E_y. A steady-state is quickly established in which the electric field E_y gives rise to a force on the electron given by:

$$eE_y = F_y \tag{7}$$

This force just balances the force due to the magnetic field.

Equating the two forces on the electrons we obtain:

$$eE_y = ev_n B_z \tag{8}$$

Assuming all the electrons have the same drift velocity the current density may be expressed as follows:

$$\bar{j}_x = ne\bar{v}_n \tag{9}$$

where the units for $\bar{j}$ are amps/meter^2 and n is the concentration of electrons/

meter^3. Substituting Equation (9) into Equation (8) and solving for the electric field E_y we obtain:

$$E_y = \frac{B_z j_x}{ne} \tag{10}$$

The Hall coefficient is defined by the following relation:[55]

$$R = \frac{E_y}{j_x B_z} \tag{11}$$

If we combine Equations (10) and (11) we obtain the following relation for the carrier concentration:

$$n = \frac{1}{Re} \tag{12}$$

It should be pointed out that when the epxression for current density was written, the assumption that all the electrons have their average drift velocity was an oversimplification of the problem. It can be shown that when the statistical distribution of the drift velocities is taken into account the following expression for carrier concentration is obtained:[56][57]

$$n = \frac{3\pi}{8} \frac{1}{Re} \tag{13}$$

This does not alter the fact that Equation (11) and Equation (12) or (13) make it possible to determine the carrier concentration from electrically measurable quantities. If a p-type bar is now substituted for the n-type the polarity of the Hall voltage reverses, since the positive holes are now driven to the top of the sample, leaving a layer of bound negative charges on the bottom of the bar. This is extremely strong evidence for the existence of positive charged holes, as well as a means of determining whether a sample is n-type or p-type.

The results just derived were for material that is either n-type or p-type. They do not hold if both types of carriers are present. If both types of carriers are present it can be shown that the Hall coefficient then has the following form:[58]

$$R = \frac{\mu_p^2 p - \mu_n^2 n}{e(\mu_p p + \mu_n n)^2} \tag{14}$$

As in Equation (13), Equation (14) is the result of an oversimplification, and we must introduce a $\frac{3\pi}{8}$ factor to correct Equation (14) also.

The Hall coefficient is the first of two important properties of semiconductors to be measured. The second is the electrical conductivity. In Figure 5 the number of electrons crossing an area perpendicular to the x direction in one second is

$$I_n = AnV_n e \tag{15}$$

where A is the area of the cross section of the sample. The current density is given by:

$$j_n = \frac{I_n}{A} \tag{16}$$

This may be written using Equation (4) as follows:

$$j_n = en\mu_n E_x \tag{17}$$

If we now combine the definition of electrical conductivity,

$$\bar{j} = \sigma \bar{E}, \tag{18}$$

with Equation (17),we obtain

$$\sigma = ne\mu_n \tag{19}$$

We see from this equation that the conductivity not only depends on carrier concentration, but that it is dependent on the mobility also. If we combine Equation (19) with Equation (12) we obtain:

$$R\sigma = \mu, \tag{20}$$

which gives the mobility expressed as the product of two measurable quantities. The mobility defined by Equation (20) is the Hall mobility, while the quantity defined by Equation (18) is called the conductivity mobility.

Hall effect measurements are generally made using the simple bar shaped sample shown in Figure 5. In making the electrical connections to the sample there are several considerations that must be fulfilled. The connections must have a low resistance and be small in size compared to the size of the sample, so as not to distrub the uniformity of the current flow. Putley[59] lists the general considerations for making good contacts to a number of the more frequently investigated semiconducting materials. It is also necessary for the sample to have a length to width ratio of at least 3:1 or even better, 4:1. The reason for this is that the current electrodes tend to short out the Hall field when the ratio becomes less than these values.

It is not always easy to make electrical connections as described above, and samples such as those shown in Figure 6 are used for Hall measurements. The side arms and enlarged areas allow large contacts to be applied without interfering with the electrical characteristics of the sample. The techniques used to make the Hall probe contact vary drastically, depending on the specimen

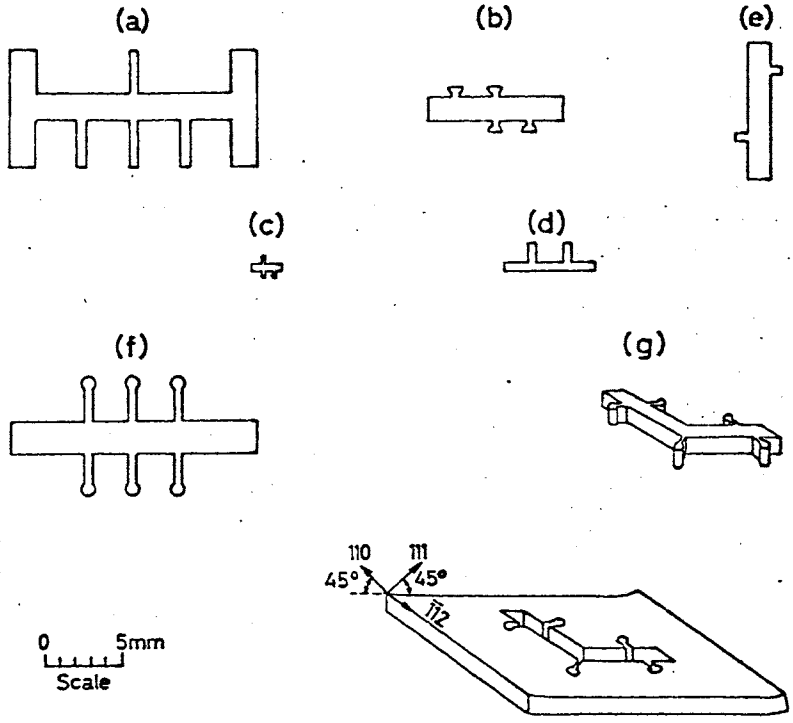

Figure 2.9. Specimen shapes drawn to approximately the same scale: (a) prepared by milling with diamond wheel; (c) and (e) sand-blasted using a mask. All others cut with ultrasonic drill. (a) Used in Dunlap's high temperature apparatus. (b) Used in Putley's high resistance cryostat. (c) Graphite single crystal (Soule). (d) Germanium thermometer element. (e) Shape used by Zemel and Petritz to study surface conduction in germanium. (f) Shape used by Bell Telephone Laboratories. (g) L-shape used at B.T.L. to investigate the effects of bending

Figure 6. Alternate sample shapes for Hall effect measurements [53]

of interest. This is a very important part of any Hall measurement, requiring a unique type contact for each different material.

The techniques[60] to produce and detect the Hall voltage are of two types: a direct current method, and an alternating current method. The latter method may also use an alternating magnetic field and a tuned amplifier to produce an output proportional to the Hall coefficient. In the direct current method a potentiometer and null detector are used to observe the Hall voltage. However, if the specimen has a resistance greater than 10^4 or 10^5 ohms, this method becomes impractical. The vibrating reed electrometer having an input resistance of the order of 10^{14} ohms may be used for measurements of high resistance samples. Alternating current methods are also used for samples having a high resistance and those developing a space charge region within the sample. The frequency of the alternating current is chosen such that a reversal of the current direction takes place before the space charge has time to form.

A bibliography of the Hall effect was prepared by Clawson and Wieder[61] and is a very useful source of information on the Hall effect and related phenomena. This paper lists almost 300 references to current literature pertinent to the theory, instrumentation, and applications of the Hall effect devices up to July 1, 1963.

III. EXPERIMENTAL PROCEDURE

A. Preparation and Heat Treating Procedure

The powder samples used in this investigation were prepared by a member of the Materials Research Center, University of Missouri-Rolla. The technique used in the preparation of these powder samples was the nitric acid leach method developed by Achenbach.[62][38] This technique has been shown to give single phase, pure $BiFeO_3$.

The heat treating procedure consisted of placing a powder of single phase $BiFeO_3$ in a platinum lined ceramic boat. The boat was then placed in a quartz furnace liner for the heat treating procedure. The furnace had previously been allowed to reach equilibrium temperature and purged of impurity atmosphere by allowing the gas being used to flow through the quartz liner for a period of at least one day. The seals of the quartz tube were not air tight, but a relatively good control of the atmosphere within the tube was obtained by merely keeping a steady flow of oxygen or nitrogen through the tube at all times during the heat treating of the samples. The temperature of the heat treating procedure was in the range of $625^{o}C$ to $680^{o}C$. The samples were heat treated for periods of from 40 hours to 5 days. After the heat treating, the powder samples were subjected to x-ray diffraction analysis using a General Electric Diffractometer, Model BR Type 1. The x-ray analysis was done before and after the heat treating procedure to ascertain whether or not either of the two impurity phases, identified by Achenbach,[62][38] were formed in the process of heating the powder.

B. Hot Pressing Procedure

The heat treated samples were next hot pressed into ceramic discs for the dielectric, electrical, and Hall effect measurements. The hot pressing technique was developed by J. P. Canner[63] of the University of Missouri-Rolla, Physics Department and was the same as used by Smith[28][64] to prepare the samples used in his high frequency investigation on $BiFeO_3$ and its perovskite solid solutions.

The powder material was first cold-pressed in a stainless steel die into a small pellet. The small pellet was then placed in a larger die in a MgO matrix for the hot pressing procedure. The hot pressing temperature was 725°C and the pressure was approximately 10,000 psi. The apparatus for this procedure was an induction heater (Ther-Monic 300A) used in conjunction with a Carver-Laboratory Press (Model B). The samples were kept at this temperature and pressure for approximately one hour, and then allowed to cool slowly to room temperature.

The excess MgO was removed and the sample ground into the required shape using silicon carbide paper (Grits 180-400).

C. Frequency Measurement Procedure

The dielectric constant and dissipation factor measurements as a function of frequency were made using two different measuring set-ups. The measurements in a range of 1 kHz to 100 kHz were made using a General Radio (Type 716-C) Capacitance Bridge in conjunction with a General Radio Unit R-C Oscillator (Type 1210-C) and a General Radio Tuned amplifier and Null Detector

(Type 1232-A). The measurements at 1 MHz were performed using a General Radio Capacitance Bridge (Type 716-CS1) in conjunction with a Hewlett Packard Test Oscillator (Type 651B), a General Radio Unit Null Detector (Type 1212-A), and a General Radio 1 MHz filter. A Boonton Radio Corporation Q-Meter (Type 260-A) was also available for checking samples at frequencies above 1 MHz.

For the measurements, the samples were ground to a fairly regular shape having two parallel surfaces. The two parallel surfaces were than given a thin coating of indium and painted with silver conducting paint. The sample was then placed between two copper electrodes for measurements using the above mentioned equipment.

D. Hall Effect Procedure

Several different sample holders and electrical circuits were tried in an attempt to carry out this phase of the research reported here. Initially we attempted to measure the Hall voltage using a Keithly Electrometer (Model 610A) and using a circuit as described by Melissinos.[65] Two problems became apparent with this set-up: first, we were unable to get a sufficient amount of current through the sample, and secondly, the Hall probe contact appeared to be rectifying in nature. It also appeared that the electrometer was too sensitive to noise for this set-up. In an attempt to eliminate the contact problem the following contacts were tried: small spots of silver paint with copper electrodes in contact with the spot, copper electrodes, chemically pointed tungsten electrodes, and indium coated platinum electrodes. It was apparent the sample resistance

was too high at room temperature, and thus a special high temperature sample holder and furnace were built to attempt the measurements.

The problem in constructing the sample holder and furnace was to build it small enough to fit in the one inch gap between the magnet pole faces. It was decided to locate the furnace below the pole pieces of the magnets and heat the sample by conduction through an aluminum cylinder resting in the furnace and extending up into the magnetic field. The aluminum furnace insert, as shown in Figure 7, is bulk material on the lower end, while the upper end which goes between the magnet pole faces and is drilled out to allow for the actual sample holder. The sample holder, shown in detail in Figure 8, was made of boron nitride, a very good thermal conductor and a highly insulating dielectric material. The vertical contacts are the current connections. The upper current connection was spring loaded and adjustable to allow for different sample sizes and thermal expansion. These contacts were stainless steel rods. The Hall probes on each side of the sample were stainless steel rods with the point contacts being made of indium coated platinum wire. Figure 9 shows the aluminum furnace insert, furnace, sample holder, and pole pieces in their assembled position.

The electrical circuit used in these measurements is shown in Figure 10. A Leeds and Northrup Type K-3 Universal Potentiometer in conjunction with a Leeds and Northrup Guarded Null Detector (Model 9834) was used to measure Hall voltages.

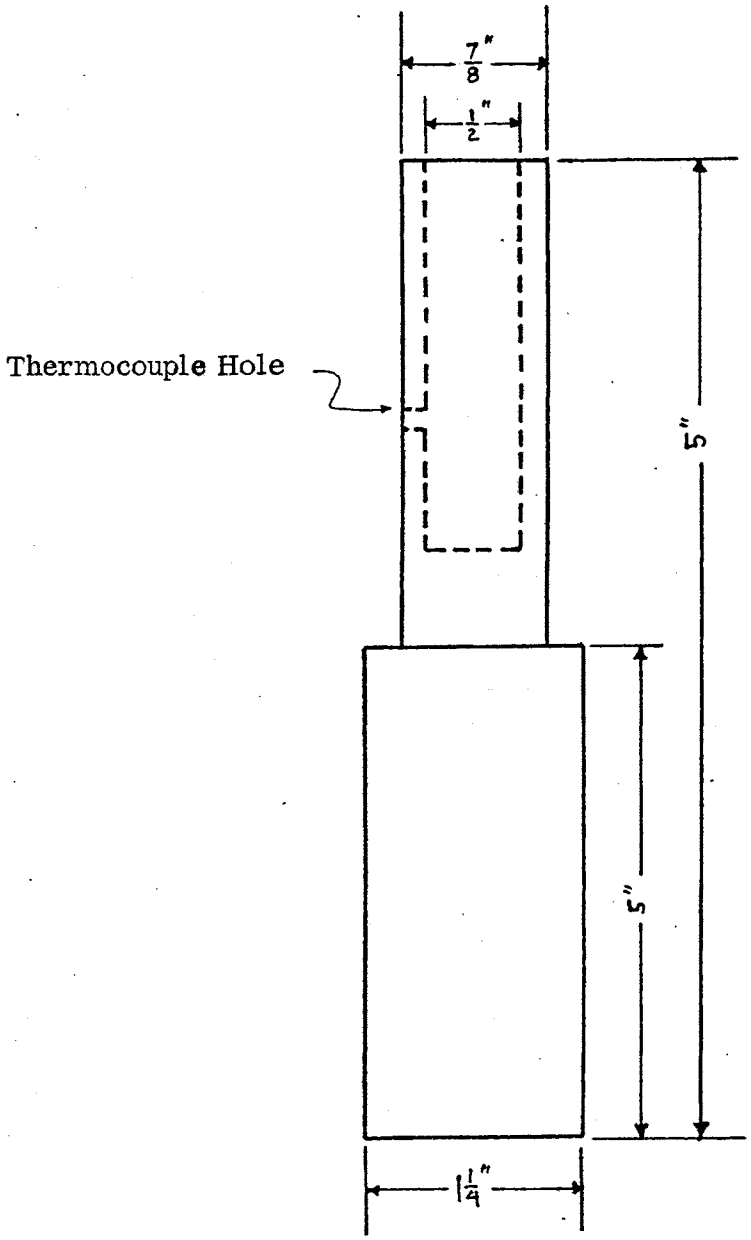

Figure 7. Aluminum furnace insert

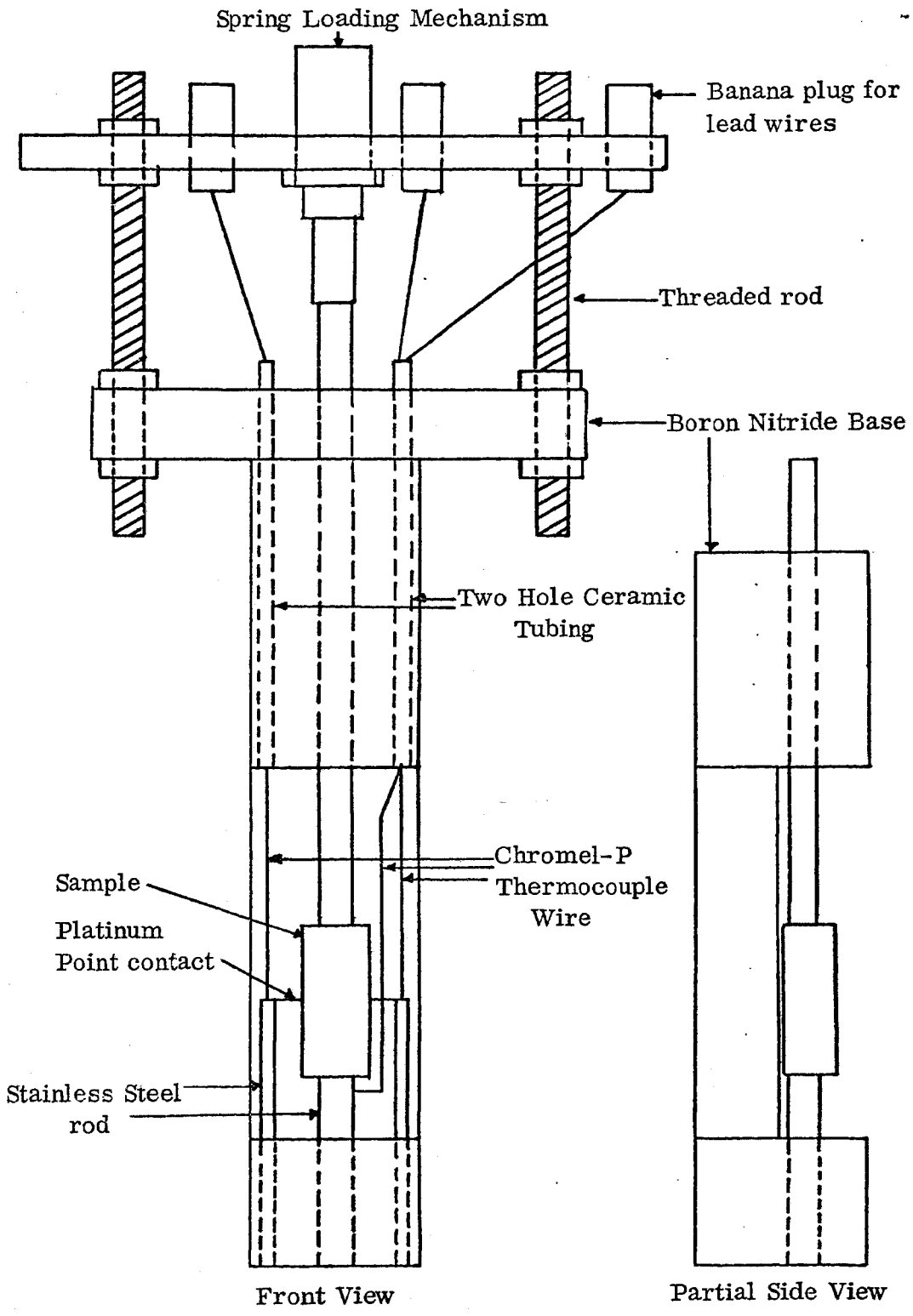

Figure 8. High temperature Hall effect sample holder

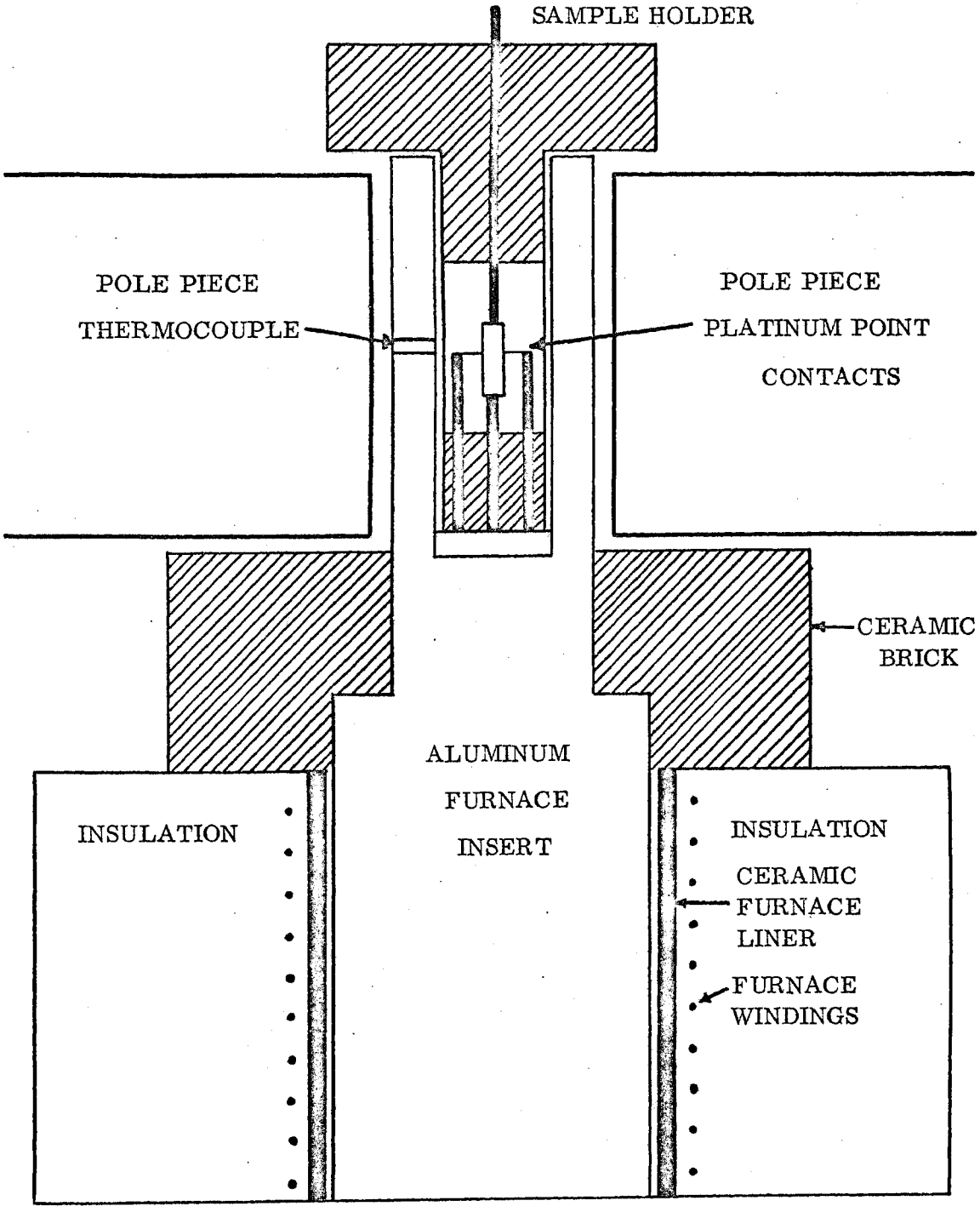

Figure 9. Hall effect apparatus employing special high temperature sample holder

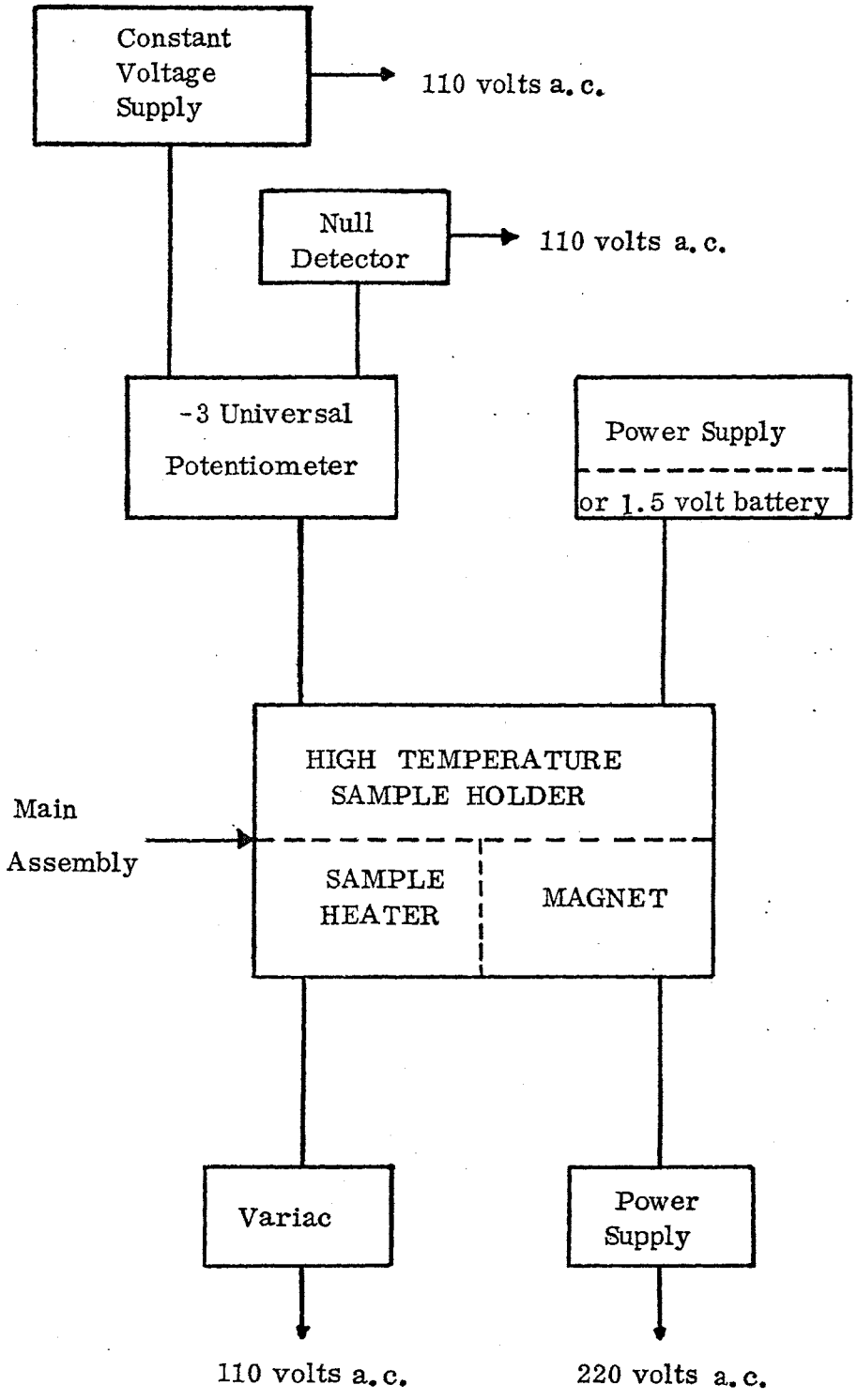

Figure 10. Block diagram of Hall effect circuit

The apparatus just described was used for two measurements; a high temperature Hall effect measurement on pure $BiFeO_3$ ceramic samples, and room temperature measurements on Ga-doped CdS single crystals. Both the $BiFeO_3$ and the CdS samples used were bar shaped as shown in Figure 5. In making the measurements on the $BiFeO_3$ the sample was allowed to reach an equilibrium temperature, between 300°C and 375°C. The higher temperature is the upper limit of this apparatus due to the melting point of the aluminum furnace insert. The current contact ends of the Hall bar were given a thin coating of indium and a coat of conducting silver paint. Using bias voltages of from 1.0 to 5.0 volts, currents of from 0.01 to 0.05 milliampswere obtained. This is the maximum current we could use without breaking down the sample at this high temperature.

The CdS samples were mounted the same as the $BiFeO_3$ samples, except for the Hall probes being indium-coated platinum point contacts. A capacitor discharge method was used to diffuse small amounts of indium into the CdS samples, thus giving ohmic contacts.

In mounting the sample it is not possible to align the Hall probes exactly opposite each other and thus there is a voltage between the Hall probes in the absence of magnetic field. This voltage arises because the unaligned probes do not lie on equipotential surfaces. To minimize the effect of this zero magnetic field voltage between the Hall probes we used the following technique in our measurements:

1. After the electric field was applied and equilibrium established, the zero field value of voltage was recorded.

2. The magnetic field was then applied and the voltage recorded.
3. The direction of the magnetic field was reversed and the voltage was recorded.
4. The above sequence of measurements was repeated several times and the results averaged.

The values of the Hall voltage were then used for the calculation of carrier concentration and mobility.

E. Resistivity Measurements

The resistivity measurements were made using three different techniques. For the CdS samples the apparatus shown in Figure 11 was constructed. The CdS samples were mounted flat in the sample holder between the two current electrodes. The two tungsten electrodes were then placed in contact with the flat surface of the sample and the contact formed. Two different types of contact proved satisfactory for these measurements. The first was plain tungsten electrodes forming the contacts by 10-15 short bursts of 18 volts of a.c. power; the second type of contact used were indium-coated tungsten electrodes, forming the contacts by 5-10 short bursts of 18 volts of a.c. power. The data for both types of contacts are shown in Tables I and II.

The current was supplied by a 1.5 volt battery and regulated by the variable resistors shown in Figure 11. A Leed and Northrup Millivolt Potentiometer was used to measure the voltage drop between the two probes. The probe separation was measured by a micrometer.

TABLE I

RESISTIVITY DATA FOR CdS SAMPLE 1

	Voltage Across Probe (millivolts)	Current Through Sample (milliamps)	Probe Separation (inches)	Resistivity (ohm·cm)
1	27.9	320	0.095	1.0×10^{-2}
2	24.6	320	0.090	0.97×10^{-2}
3	22.9	310	0.090	0.94×10^{-2}
4	25.5	320	0.090	0.96×10^{-2}
	Sample Area = .0290 cm^2 for measurements 1 - 4			
5	22.5	290	0.081	0.98×10^{-2}
6	26.2	300	0.090	0.99×10^{-2}
7	25.4	310	0.090	0.93×10^{-2}
8	24.8	295	0.090	0.96×10^{-2}
	Sample Area = .026 cm^2 for measurements 5 - 8			

NOTE: Measurements 1 - 4 were made using indium coated tungsten electrodes, while 5-8 were made using uncoated tungsten electrodes. Measurements 1 - 4 were made on the opposite side of the sample from the side used for 5 - 8.

Current direction was along c-axis of crystal.

TABLE II

RESISTIVITY DATA FOR CdS SAMPLE 2

	Voltage Across Probes (millivolts)	Current Through Sample (milliamps)	Probe Separation (inches)	Resistivity (ohm·cm)
1	21.9	65.0	0.25	1.3×10^{-2}
2	20.8	66.0	0.25	1.3×10^{-2}
	Sample turned over.			
3	19.5	62.0	0.25	1.2×10^{-2}
4	20.5	62.0	0.25	1.2×10^{-2}
	Measurements 1 - 4 made previous to Run 1 for Hall effect.			
5	21.6	66.0	0.25	1.2×10^{-2}

Measurement 5 made previous to Run 2 for Hall effect.

Sample area = .024 cm^2 for measurements 1 - 5
Current direction parallel to c-axis of crystal

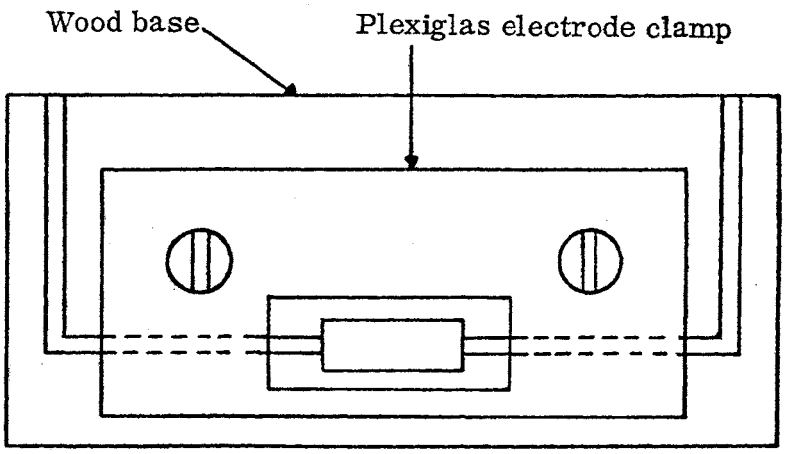

Partial Top View

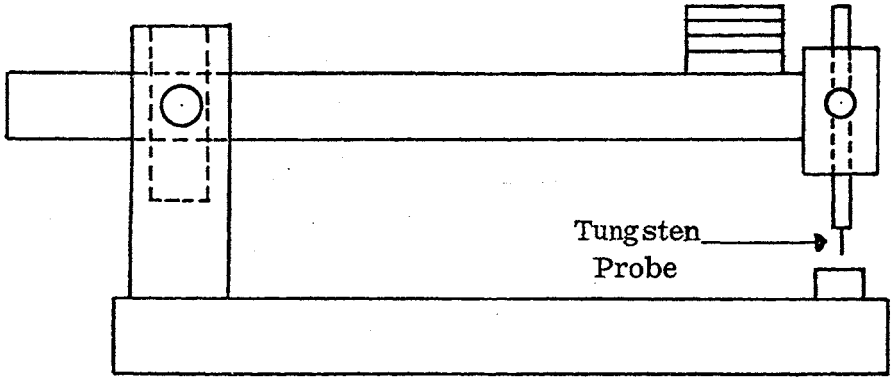

Side View

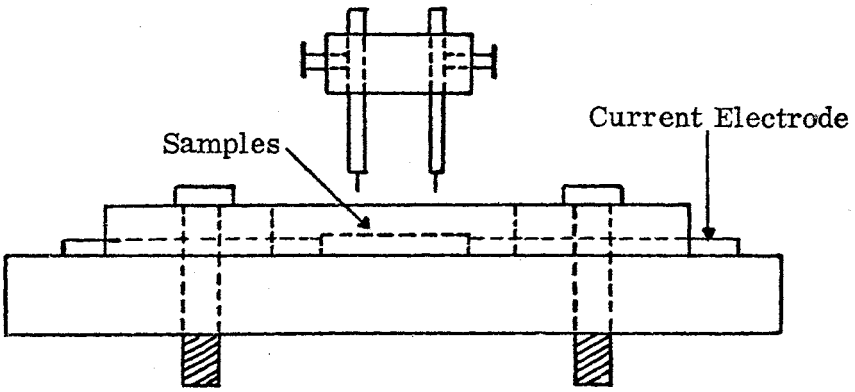

Front View

Figure 11. Modified 4-point resistivity apparatus

This technique proved unsatisfactory for the $BiFeO_3$ samples. Neither the plain or indium coated electrodes could be formed for the $BiFeO_3$. Both a.c. and d.c. techniques were attempted, but both produced a burned area directly beneath the electrode before a contact was formed. The results given in Table III were obtained by applying a voltage to the sample and measuring the current flowing through the sample. This data and the sample dimensions were then used to calculate the resistivity values reported here. The resistivity versus temperature data given in Tables IV and V were obtained in this manner with the sample mounted in the high temperature Hall effect sample holder.

F. Hot-Point Probe Procedure

The Hall effect is not the only method of determining the conductivity type of a semiconductor. The conductivity type may also be established by the hot-point probe method. The experimental set-up, as given by Gibbons, [66] is shown in Figure 12. A Hewlett Packard microvolt-ammeter (Model 425-A) was the high impedance voltmeter used in this work. Measurements were made with the soldering iron turned off to avoid a.c. pickup. The sign of the voltage measured is the sign of the carriers present.

TABLE III

RESISTIVITY AS A FUNCTION OF BIASING VOLTAGE

FOR $BiFeO_3$ SAMPLES

Bias Voltage = 10 volts

	Current (amps)	Resistivity (ohm·cm)
Sample 1	3.8×10^{-6}	2.3×10^{6}
Sample 2	3.6×10^{-6}	2.1×10^{6}
Sample 3	3.6×10^{-6}	2.1×10^{6}
Sample 4	1.2×10^{-6}	9.5×10^{5}
Sample 5	5.8×10^{-5}	4.1×10^{5}
Sample 6	1.4×10^{-5}	1.5×10^{6}

Bias Voltage = 20 volts

	Current (amps)	Resistivity (ohm·cm)
Sample 1	1.7×10^{-5}	1.0×10^{6}
Sample 2	1.5×10^{-5}	1.0×10^{6}
Sample 3	8.8×10^{-5}	1.8×10^{6}
Sample 4	5.5×10^{-5}	4.3×10^{5}
Sample 5	2.0×10^{-4}	2.4×10^{5}
Sample 6	5.1×10^{-5}	8.4×10^{5}

Bias Voltage = 30 volts

	Current (amps)	Resistivity (ohm·cm)
Sample 1	3.6×10^{-5}	7.3×10^{5}
Sample 2	3.2×10^{-5}	6.9×10^{5}
Sample 3	1.8×10^{-4}	1.3×10^{6}
Sample 4	3.9×10^{-5}	3.1×10^{5}
Sample 5	4.1×10^{-4}	1.7×10^{5}
Sample 6	1.2×10^{-4}	5.3×10^{5}

TABLE III (CONTINUED)

RESISTIVITY AS A FUNCTION OF BIASING VOLTAGE

FOR $BiFeO_3$ SAMPLES

Bias Voltage = 40 volts

	Current (amps)	Resistivity (ohm·cm)
Sample 1	6.5×10^{-5}	5.3×10^{5}
Sample 2	6.0×10^{-5}	5.0×10^{5}
Sample 3	3.1×10^{-4}	1.0×10^{6}
Sample 4	2.9×10^{-5}	2.3×10^{5}
Sample 5	7.6×10^{-4}	1.6×10^{5}
Sample 6	2.4×10^{-4}	3.5×10^{5}

Bias Voltage = 50 volts

	Current (amps)	Resistivity (ohm·cm)
Sample 1	1.1×10^{-4}	3.9×10^{5}
Sample 2	1.0×10^{-4}	3.6×10^{5}
Sample 3	4.9×10^{-4}	7.9×10^{5}
Sample 4	3.4×10^{-5}	1.9×10^{5}
Sample 5	1.7×10^{-3}	7.1×10^{4}
Sample 6	3.9×10^{-4}	2.7×10^{5}

TABLE IV

RESISISTIVITY VERSUS TEMPERATURE DATA FOR $BiFeO_3$ SAMPLE 1

Temperature (^{o}C)	Voltage Drop Across Samples (volts)	Current Through Sample (amps)	Resistivity (ohm·cm)
150	10	6.5×10^{-8}	1.0×10^{7}
168	10	9.6×10^{-8}	6.7×10^{6}
191	10	2.3×10^{-7}	2.8×10^{6}
205	10	4.1×10^{-7}	1.1×10^{6}
220	10	6.6×10^{-7}	9.9×10^{5}
237	10	1.0×10^{-6}	6.6×10^{5}
258	10	3.0×10^{-6}	2.1×10^{5}
273	10	4.5×10^{-6}	1.4×10^{5}
291	10	7.1×10^{-6}	9.2×10^{4}
301	10	9.5×10^{-6}	6.9×10^{4}
Sample breaks down at approximately 300°C for 10 volts bias.			
274	1.43	2.8×10^{-7}	3.3×10^{5}
286	1.43	6.1×10^{-7}	1.5×10^{5}
295	1.43	9.4×10^{-7}	9.9×10^{4}
300	1.43	1.1×10^{-6}	8.0×10^{4}
310	1.43	1.4×10^{-6}	6.6×10^{4}

TABLE IV (CONTINUED)

RESISTIVITY VERSUS TEMPERATURE DATA FOR $BiFeO_3$ SAMPLE 1

Temperature (^{o}C)	Voltage Drop Across Samples (volts)	Current Through Sample (amps)	Resistivity (ohm·cm)
319	1.43	2.5×10^{-6}	3.7×10^{4}
329	1.43	4.9×10^{-6}	1.9×10^{4}
340	1.43	1.0×10^{-5}	8.4×10^{3}
355	1.43	1.2×10^{-5}	7.8×10^{3}
364	1.43	1.3×10^{-5}	6.9×10^{3}
376	1.43	1.6×10^{-5}	5.8×10^{3}

TABLE V

RESISTIVITY VERSUS TEMPERATURE DATA FOR $BiFeO_3$ SAMPLE 4

Temperature (^{o}C)	Voltage Drop Across Samples (volts)	Current Through Sample (amps)	Resistivity (ohm·cm)
180	10.0	3.0×10^{-7}	2.4×10^{6}
197	10.0	4.0×10^{-7}	1.8×10^{6}
240	10.0	2.8×10^{-6}	2.6×10^{5}
255	10.0	5.6×10^{-6}	1.3×10^{5}
262	10.0	9.0×10^{-6}	8.2×10^{4}
272	10.0	1.3×10^{-5}	5.7×10^{4}
283	10.0	1.8×10^{-5}	4.1×10^{4}
299	10.0	2.5×10^{-5}	2.9×10^{4}
Sample breaks down at approximately $300^{o}C$ for 10 volts bias.			
275	1.43	8.0×10^{-7}	1.3×10^{-5}
280	1.43	9.6×10^{-7}	1.1×10^{5}
290	1.43	1.5×10^{-6}	7.2×10^{4}
305	1.43	2.5×10^{-6}	4.3×10^{4}
316	1.43	3.7×10^{-6}	2.9×10^{4}
327	1.43	5.7×10^{-6}	1.9×10^{4}
332	1.43	7.1×10^{-6}	1.5×10^{4}

TABLE V (CONTINUED)

RESISTIVITY VERSUS TEMPERATURE DATA FOR $BiFeO_3$ SAMPLE 4

Temperature (^{o}C)	Voltage Drop Across Samples (volts)	Current Through Sample (amps)	Resistivity (ohm·cm)
338	1.43	8.6×10^{-6}	1.2×10^{4}
346	1.43	1.2×10^{-5}	9.0×10^{3}
353	1.43	1.6×10^{-5}	6.7×10^{3}
361	1.43	2.3×10^{-5}	4.7×10^{3}
371	1.43	3.2×10^{-5}	3.4×10^{3}
376	1.43	4.0×10^{-5}	2.7×10^{3}

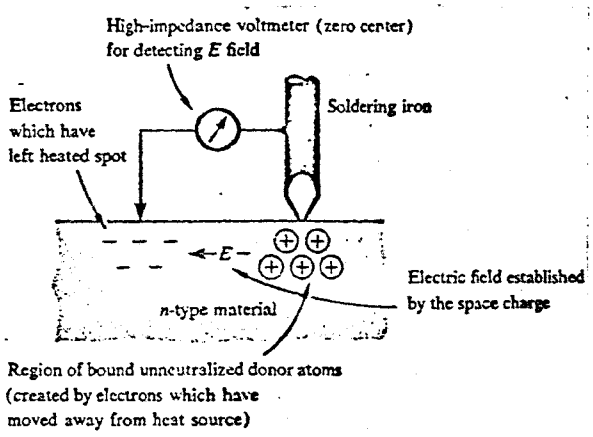

(a) *An n-type sample*

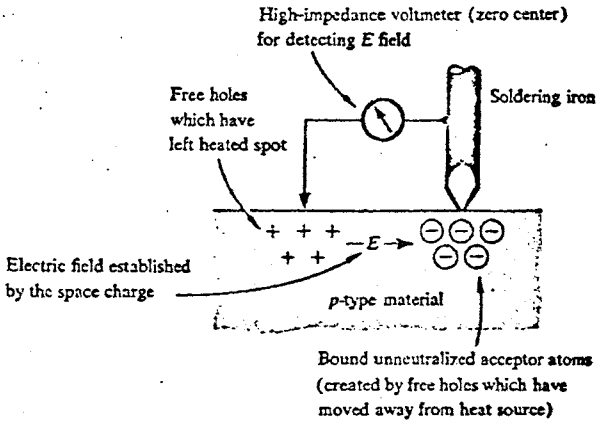

(b) *A p-type sample*

Figure 12. Hot-Point Probe measurements for n-type and p-type materials [66]

IV. DISCUSSION OF RESULTS

The results of the investigation into the effect of heat treating $BiFeO_3$ in various atmospheres were inconclusive.

The heat treatments were first done in an oxygen (oxidizing) atmosphere. The powder sample of $BiFeO_3$ was first treated for 40 hours at $625^{o}C$. X-ray analysis, performed after this heat treatment, established that the single phase nature of the sample had remained unchanged. After hot pressing, the dielectric constant and dissipation factor at 1 KHz and 10 KHz were not significantly different from earlier results for untreated samples. The sample was subsequently heat treated two more times (50 hours each) in an oxygen atmosphere at $625^{o}C$ and $680^{o}C$, but the sample still failed to show a marked change in dielectric constant and dissipation factor. Measurements at 100 KHz indicated a dissipation factor greater than 100%. The results of the measurements at 1 KHz and 10 KHz are listed in Table VI as Sample 1-a, Sample 1-b, and Sample 1-c respectively. This same sample was next heat treated for 72 hours at $650^{o}C$ in a nitrogen (reducing) atmosphere, and this process made a definite change in the sample. The low frequency results obtained after this treatment are given in Table VI (under the heading Sample 6-d). Dielectric constant and dissipation factor as a function of temperature for this sample, along with those obtained by Canner for pure $BiFeO_3$, are given in Figure 13.

The high values of the dielectric constant in Table VI are due to the blocking electrodes formed by the silver paint. At high frequency the value of the dielectric constant reduces to approximately 60. The non-linearity of the

TABLE VI

DIELECTRIC CONSTANT AND DISSIPATION FACTOR AS A FUNCTION OF FREQUENCY FOR SAMPLE 6 - $BiFeO_3$

	Frequency (Hz.)	Dielectric Constant	Dissipation Factor
Sample 6-a	10^3	5280	16.6%
	10^4	4280	30.7%
Sample 6-b	10^3	8030	31.8%
	10^4	5230	38.8%
Sample 6-c	10^3	6590	31.1%
	10^4	4260	42.7%
Sample 6-d	10^3	3220	60.6%
	10^4	402	117%

NOTE: This is not four separate samples a, b, c, and d indicate a progression of heat treatments.

TABLE VII

SUMMARY OF HEAT TREATMENTS FOR $BiFeO_3$ SAMPLES

	Atmosphere	Temperature	Duration	X-ray Results
Sample 1	oxygen	625°C	40 hours	single phase
Sample 2	oxygen	625°C	40 hours	single phase
Sample 3	-- no heating --			single phase
Sample 4	nitrogen	655°C	120 hours	multiple phase
Sample 5	nitrogen	655°C	120 hours	multiple phase
Sample 6-a	oxygen	625°C	40 hours	single phase
Sample 6-b	oxygen	625°C	50 hours	unknown
Sample 6-c	oxygen	680°C	50 hours	unknown
Sample 6-d	nitrogen	650°C	72 hours	unknown

NOTE: Samples 6-a, b, c, and d are one and the same sample.

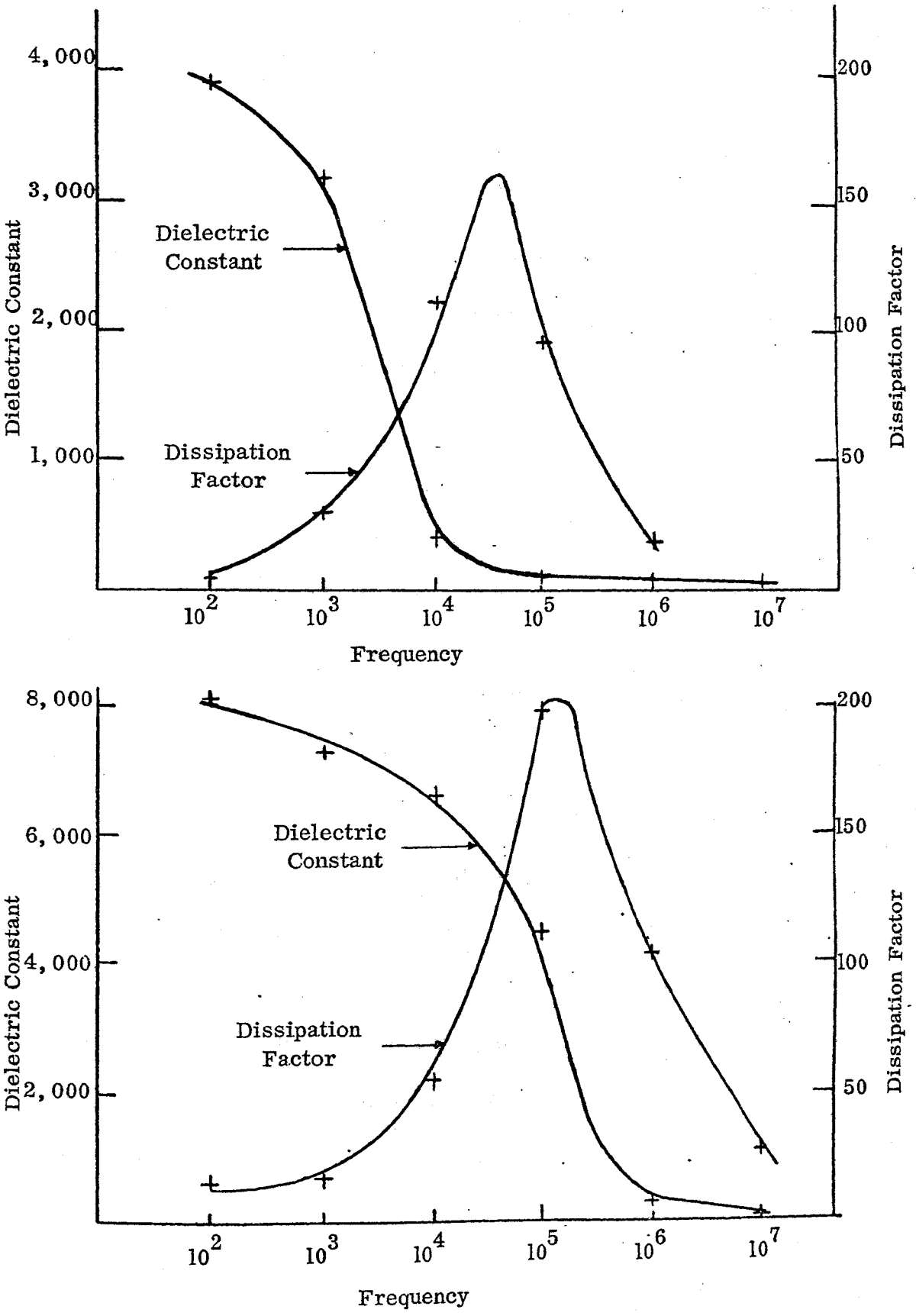

Figure 13. Dielectric constant and dissipation factor as a function of frequency

resistivity versus bias voltage curves is another result of the blocking electrodes. Figure 14 shows this non-linearity for both a nitrogen and oxygen sample and is typical of the behavior demonstrated by all six samples in Table III. It should be noted that the resistivity values for the $BiFeO_3$ samples were not obtained using a 4-point method. They are only an indication of the true resistivity. However, the values obtained are useful for comparison of the different samples.

Two subsequent samples were heat treated in a nitrogen atmosphere for 120 hours at 655°C. The x-ray analysis of these two samples reveals the presence of the impurity phases $Bi_2Fe_4O_9$ and Bi_2O_3. It appears that Sample 6-d also may have contained these impurities to a minor extent.

The resistivity as a function of bias voltage given in Table III also supports the contention, that Sample 6-d had impurity phases present. Samples 4, 5, and 6 have all been heat treated in nitrogen and they all have resistivity values somewhat lower than the oxygen treated and untreated samples. The suspicion that the oxygen heat treating was not altering the samples is supported by the approximate equality of the resistivity of Samples 1, 2, and 3. The resistivity as a function of temperature data given in Tables IV and V was used in the Hall effect analysis. These results, illustrated in Figures 15 and 16, also show a slightly lower resistivity for nitrogen heat treated samples. The lower resistivity values of the nitrogen heat treated samples and the higher dissipation factors are consistent in results, but no explanation for this is offered at this time.

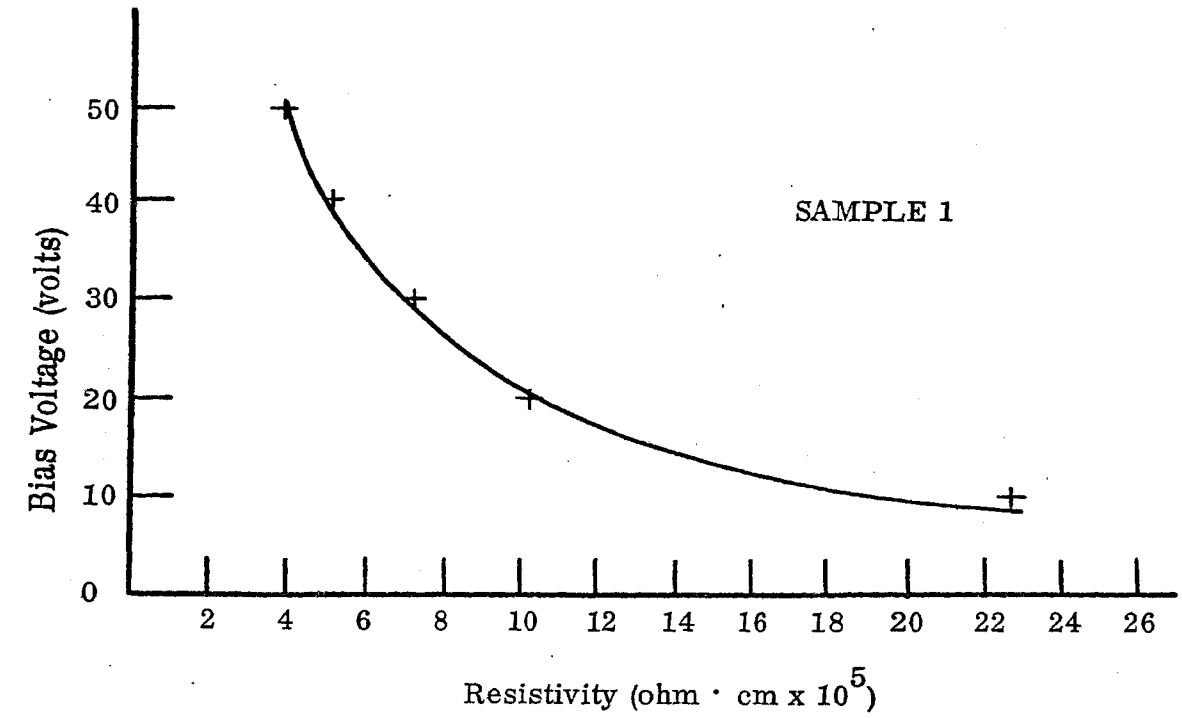

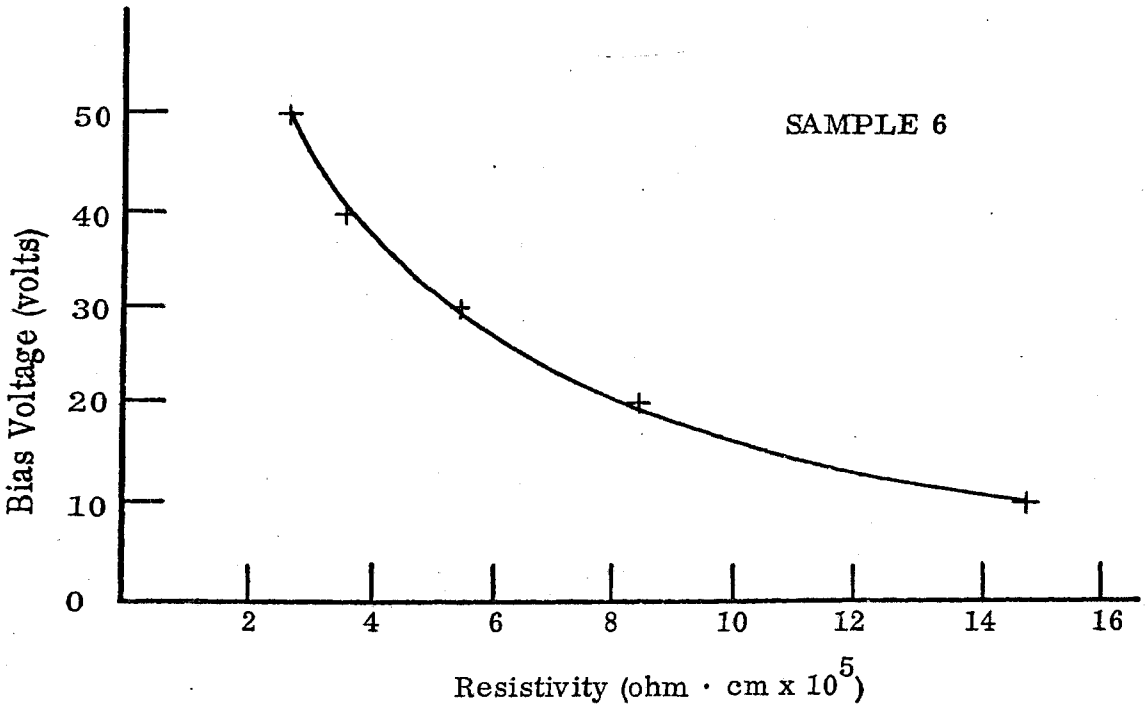

Figure 14. Resistivity as a function of bias voltage for typical heat treated $BiFeO_3$ samples

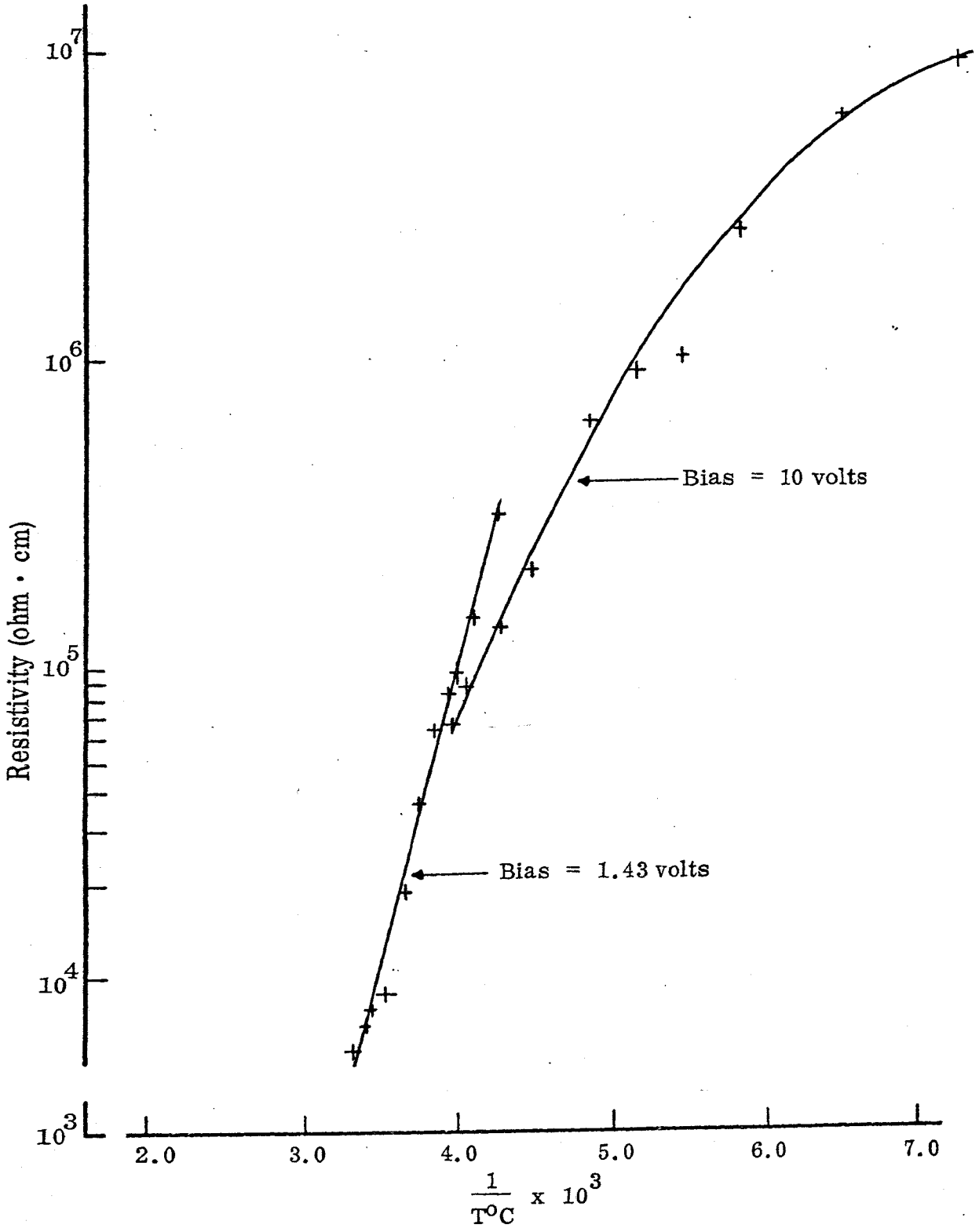

Figure 15. Resistivity as a function of temperature for $BiFeO_3$, Sample 1

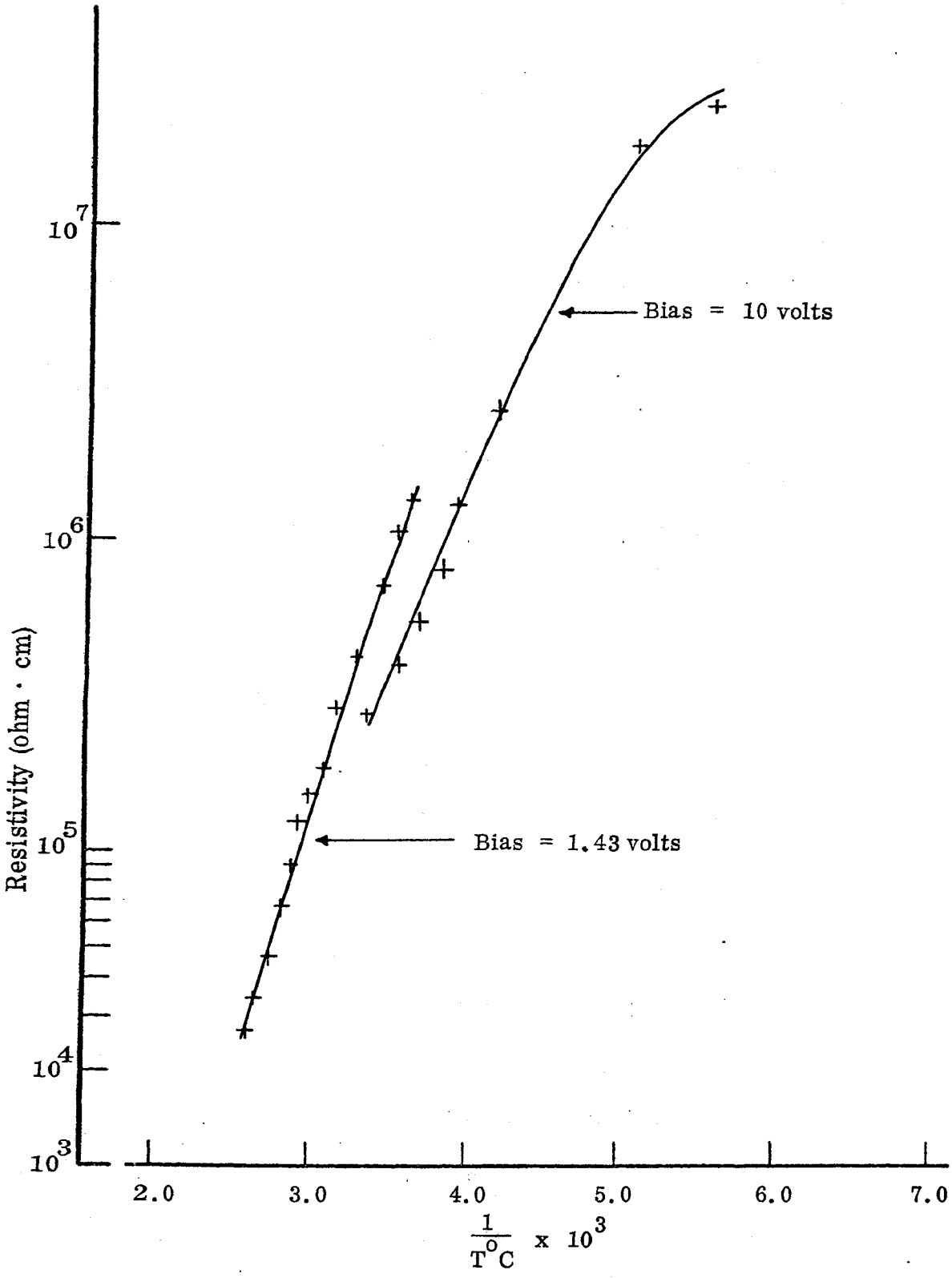

Figure 16. Resistivity as a function of temperature for $BiFeO_3$, Sample 4

The apparatus described in Section III-D was used to measure the Hall voltage in two samples of $BiFeO_3$ and two samples of CdS. The $BiFeO_3$ samples used were Sample 1 (oxygen heat treatment) and Sample 4 (nitrogen heat treatment). The details of the heat treatments these samples underwent are given in Table VII. These samples were mounted in the high temperature sample holder, and measurements attempted at temperatures in the range from 300°C to 376°C. Measurements in the temperature range 25°C to 300°C were impossible because of the high sample resistance. The apparatus became increasingly sensitive in the temperature range of 300°C to 375°C, and a fairly good balance was obtained at 375°C. At 375°C, the application of the magnetic field (5800 gauss) failed to produce a detectable Hall voltage. Subsequent measurements, using Hall bars of CdS showed the equipment to be sensitive to signals of 80 microvolts. The equipment could probably detect differences as small as 10 to 20 microvolts in the $BiFeO_3$ samples. If the 20 microvolt value is used, the values of Hall mobility become approximately .2cm^2/volt second and .6cm^2/volt second for Samples 1 and 4 at 375°C. Since the Hall voltage was actually less than 20 microvolts, it was concluded that the Hall mobility for $BiFeO_3$ was less than 0.5cm^2/volt second.

The absence of a detectable Hall voltage precludes the possibility of determining the type of conductivity present. The Hot-Point Probe measurements described in Section III-F were carried out for this reason. The signals detected in these measurements were of the order of 10^{-4} volts. The six samples described in Table VII were all tested. Four of the Samples (1, 3, 4, and 5)

demonstrated p-type conductivity, one sample (2) demonstrated n-type conductivity, and one sample (6) failed to give a detectable reading. These results tend to indicate that $BiFeO_3$ is a p-type conductor. This would not invalidate the assumption that d-electrons are responsible for the conduction in $BiFeO_3$. Conduction by d-electrons may be either n-type or p-type.

The results of the Hall effect measurements on the two samples of CdS were much more conclusive than for the $BiFeO_3$ samples. Using the technique outlined in Section III-D, the data shown in Tables VII, VIII, IX, and X were compiled. This data and the results of resistivity measurements given in Tables I and II were used to calculate carrier concentrations and Hall mobilities. A summary of the results obtained for the CdS samples is given in Table XII. The sign of the Hall voltage indicated both samples were n-type semi-conductors.

These results also indicated that a workable sample holder and accompanying instrumentation had been assembled, and this permitted us to calculate the limit on the Hall mobility for $BiFeO_3$.

TABLE VIII

HALL EFFECT DATA FOR CdS SAMPLE 1, RUN 1

Magnetic Field Strength And Direction (Gauss)	Voltage Across Hall Probes (volts)	Hall Voltage (Volts)
off	.000858	.000081
5800 Forward	.000777	
off	.000856	.000079
off	.000851	.000082
5800 Reverse	.000933	
off	.000850	.000081
off	.000845	.000081
5800 Forward	.000764	
off	.000840	.000076
off	.000850	.000082
5800 Reverse	.000932	
off	.000847	.000079
off	.000851	.000081
5800 Forward	.000770	
off	.000853	.000083
off	.000850	.000082
5800 Reverse	.000932	
off	.000851	.000081

TABLE VIII (CONTINUED)

HALL EFFECT DATA FOR CdS SAMPLE 1, RUN 1

Magnetic Field Strength And Direction (Gauss)	Voltage Across Hall Probes (Volts)	Hall Voltage (Volts)
off	.000853	.000078
5800 Forward	.000775	
off	.000855	.000080
off	.000851	.000081
5800 Reverse	.000930	
off	.000850	.000080

Average Hall voltage = $(80 \pm 2) \times 10^{-6}$ volts

Distance between Hall probes = .189 cm.

Current Density = 7.04 x 104 amps/meter^2

HALL EFFECT DATA FOR CdS SAMPLE 1, RUN 2

Magnetic Field Strength And Direction (Gauss)	Voltage Across Hall Probes (Volts)	Hall Voltage (Volts)
off	.000822	.000082
5800 Forward	.000740	
off	.000823	.000081
off	.000821	.000082
5800 Reverse	.000903	
off	.000822	.000081
off	.000824	.000083
5800 Forward	.000741	
off	.000823	.000082
off	.000820	.000080
5800 Reverse	.000900	
off	.000811	.000082
off	.000821	.000083
5800 Forward	.000738	
off	.000821	.000083

TABLE IX (CONTINUED)

HALL EFFECT DATA FOR CdS SAMPLE 1, RUN 2

Magnetic Field Strength And Direction (Gauss)		Voltage Across Hall Probes (Volts)	Hall Voltage (Volts)
off		.000820	.000081
5800	Reverse	.000901	
off		.000818	.000083

Average Hall voltage = $(82 \pm 1) \times 10^{-6}$ volts

Distance Besteen Hall Probes = .189 cm.

Current Density = 6.91×10^{4} amps/meter^{2}

NOTE: Sample was removed and remounted between Run 1 and Run 2

HALL EFFECT DATA FOR CdS SAMPLE 2, RUN 1

Magnetic Field Strength And Direction (Gauss)	Voltage Across Hall Probes (Volts)	Hall Voltage (Volts)
off	.000270	.000093
5800 Forward	.000177	
off	.000270	.000093
off	.000270	.000092
5800 Reverse	.000362	
off	.000273	.000089
off	.000271	.000091
5800 Forward	.000180	
off	.000272	.000090
off	.000273	.000088
5800 Reverse	.000361	
off	.000271	.000090
off	.000269	.000090
5800 Forward	.000179	
off	.000269	.000090
off	.000270	.000091
5800 Reverse	.000361	
off	.000269	.000092

TABLE X (CONTINUED)

HALL EFFECT DATA FOR CdS SAMPLE 2, RUN 1

Magnetic Field Strength And Direction (Gauss)		Voltage Across Hall Probes (Volts)	Hall Voltage (Volts)
off		.000271	.000092
5800	Forward	.000179	
off		.000270	.000091
off		.000271	.000092
5800	Reverse	.000363	
off		.000272	.000091

Average Hall voltage = $(91 \pm 1) \times 10^{-6}$ volts

Distance Between Hall Probes = .245 cm.

Current Density = 1.23×10^{4} amps/meter^{2}

TABLE XI

HALL EFFECT DATA FOR CdS SAMPLE 2, RUN 2

Magnetic Field Strength And Direction (Gauss)	Voltage Across Hall Probes (Volts)	Hall Voltage (Volts)
off	.000253	.000085
5800 Forward	.000168	
off	.000250	.000082
off	.000254	.000083
5800 Reverse	.000337	
off	.000252	.000083
off	.000256	.000081
5800 Forward	.000337	
off	.000257	.000080
off	.000251	.000084
5800 Reverse	.000167	
off	.000253	.000086

Average Hall Voltage = $(84 \pm 2) \times 10^{-6}$ volts

Distance Between Hall Probes = .245 cm.

Current Density = 1.21×10^{4} amps/meter^{2}

TABLE XII

SUMMARY OF CdS HALL EFFECT RESULTS

	Carrier Concentration (carriers/meter^3)	Hall Coefficient (meter^3/coulomb)	Hall Mobility (meter^3/volt·sec)
Sample 1 - Run 1	6.1×10^{24}	1.0×10^{-6}	1.1×10^{2}
Sample 1 - Run 2	5.8×10^{24}	1.1×10^{-6}	1.1×10^{2}
Sample 2 - Run 1	1.2×10^{24}	5.1×10^{-6}	4.2×10^{2}
Sample 2 - Run 2	1.3×10^{24}	4.9×10^{-6}	4.0×10^{2}

Resistivity = 0.96×10^{-4} ohm·meter for sample 1

Resistivity = 1.2×10^{-4} ohm·meter for sample 2

V. CONCLUSIONS

This investigation shows that heat treating samples of $BiFeO_3$ in oxygen does not reduce the conductivity, while heat treating in nitrogen yields samples with the impurity phase present. These impure samples have a lower conductivity, but this may be due to the presence of the impurity phases. These results do not invalidate the postulate that the presence of Fe^{++} is responsible for the conductivity of $BiFeO_3$.

The results (undetectable Hall voltage) of the high temperature Hall effect measurements implied that the Hall mobility for $BiFeO_3$ was less than .5 cm^2/ volts second. Hot-Point Probe (thermoelectric) results tended to indicate that $BiFeO_3$ has p-type conductivity, but all samples tested were not consistent.

The results of the Hall effect measurement on CdS are summarized in Table XII. The samples were shown to be n-type semi-conductors. The CdS results also demonstrated that a workable Hall effect sample holder and accompanying instrumentation had been constructed.

BIBLIOGRAPHY

(1) J. Valasek, Phys. Rev. 20, 639 (1922).

(2) H. D. Megaw, Ferroelectricity in Crystals (Methuen and Co., Ltd., London, 1957), p. 14.

(3) C. Kittel, Introduction to Solid State Physics (John Wiley and Sons, Inc., New York, 1956), 2nd ed., p. 186.

(4) J. C. Burfoot, Ferroelectrics: An Introduction to Physical Principles (D. Von Nostrand Co., Ltd., London, 1967) p. 1.

(5) F. Jona and G. Shirane, Ferroelectric Crystals (The MacMillan Co., 1962) p. 10.

(6) E. Fatuzzo and W. J. Merz, Ferroelectricity (John Wiley and Sons., Inc., New York, 1967) pp. 5-6.

(7) J. C. Burfoot (1967), op. cit., p. 2.

(8) F. Jona and G. Shirane (1962), op. cit. pp. 10-11.

(9) J. C. Burfoot (1967), op. cit., p. 7.

(10) F. Jona and G. Shirane (1962), op. cit. pp. 11-13.

(11) C. Kittel (1956), op. cit., p. 13.

(12) H. D. Megaw (1957), op. cit., p. 13.

(13) H. D. Megaw (1957, op. cit., p. 14.

(14) C. Kittel, Introduction to Solid State Physics (John Wiley and Sons, Inc., New York, 1967) 3rd ed., pp. 407-409.

(15) C. Kittel (1956), op. cit., pp. 186, 205.

(16) C. Kittel, Phys. Rev., 82, 729 (1951).

(17) H. D. Megaw (1957), op. cit., p. 16.

(18) I. Nara-Szabo, Muegyetemi Kozlemenyek 1947, No. 1, 30-41, (1947).

(19) H. D. Megaw, Proc. Phys. Soc. (London) 58, 10, (1946).

(20) R. S. Roth, Journal of Research, Nat. Bureau of Standards 58, 10, (1946).

(21) H. D. Megaw (1957), op. cit., pp. 86-87.

(22) V. M. Goldschmidt, Skrifter Norske Videnskaps-Akad Mat. Naturvid kl, 2, (1926).

(23) M. L. Keith and R. Roy, The Amer. Mineralogist 39, 1 and 2, 1, (1954).

(24) V. M. Goldschmidt, Skrift Norske Vidensak. Akad., No. 2, 8, (1926).

(25) H. D. Megaw (1957), op. cit., p. 83.

(26) B. T. Matthias, Science 113, 591, (1951).

(27) R. T. Smith, doctoral dissertation, University of Missouri at Rolla (1967).

(28) J. I. Latham, doctoral dissertation, University of Missouri at Rolla (1967).

(29) V. S. Filipev, N. P. Smolyaninov, E. G. Fesenko, and I. N. Belyaev, Soviet Physics-Crystallography 5, 913, (1960).

(30) Yu. Venevstev, G. Zhdanov, S. Solovev, E. Bezus, V. Ivanova, S. Fedulov, and A. Kapyshev, Soviet Physics-Crystallography 5, 594-599, (1961).

(31) A. I. Zaslavskii and A. G. Tutov, Soviet Phys.-Doklady 135, 1257, (1960).

(32) Yu. Ya. Tomashpol' skii, Yu N. Venevstev, and G. S. Zhdanov, Sovite Physics-Doklady 8, 1144, (1964).

(33) S. A. Fedulov, Yu. N. Venevtsev, G. S. Zhdanov and E. G. Smazhevskaya, Soviet Physics-Crystallography 6, 795, (1961).

(34) S. A. Fedulov, Soviet Physics-Doklady 6, 729, (1962).

(35) S. V. Kiselev, A. N. Kshnjkina, R. P. Ozerov, and G. S. Zhdanov, Soviet Physics - Solid State 5, 11, 2425, (1964).

(36) V. P. Plakhtii, E. I. Maltsev, and D. M. Kaminker, Bul of Acad. of Sciences, USSR, Phys. Series 28; 1-6, 350, ((1964).

(37) Y. E. Roginskaya, Y. Y. Tomashpol' skii, Y. N. Venevstev, V. M. Petrov, and G. S. Zhdanov, Soviet Physics 0 JETP 23, 1, 49, (1966).

(38) G. D. Achenbach, masters thesis, University of Missouri at Rolla (1967).

(39) G. A. Smolenskii, V. M Yudin, E. S. Shur, and Y. E. Stolypin, Soviet Physics - JETP 16, 622, (1963).

(40) V. M. Yudin, Bul. Acad. of Science, USSR, Phys. Series 28, 1-6, 363-364, (1964).

(41) V. M. Yudin, Soviet Physics - Solid State 8, 1, 217-218, (1966).

(42) S. V. Kiselev, R. P. Ozerov, and G. S. Zhdanov, Soviet Physics-Doklady 1, 8, 742, (1963).

(43) B. A. Banks, masters thesis, University of Missouri at Rolla (1965).

(44) N. N. Krainik, N. P. Kuchua, V. V. Zhdanova, and V. A. Evseev, Soviet Phys. - Solid State 8, 654 (1966).

(45) N. N. Krainik, N. P. Kuchua, A. A. Berezhnoi, A. G. Tutov, and A. Yu. Cherkashckenko, Bull. Acad. Sci. USSR Phys. Ser. 29, 1025 (1965).

(46) G. A. Smolenskii, and V. M. Yudin, Soviet Physics-Solid State 6, 12, 2936-38 (1965).

(47) Yu. Ya. Tomashpol' skii, Yu. N. Venevtsev, and G. S. Zhdanov, Soviet Phys.-JETP 19, 1294 (1964).

(48) R. W. Smith, Phys. Rev. 97, 1525 (1955).

(49) F. A. Kroger, G. Diemer, and H. A. Klasens, Phys. Rev. 103, 279 (1956).

(50) C. Kittel (1967), op. cit., pp. 199-297.

(51) E. H. Hall, Amer. J. Math 2, 287 (1879).

(52) C. Kittel (1956), op. cit., pp. 296-298.

(53) E. H. Putley, The Hall Effect and Related Phenomena (Butterworths and Co., Ltd., London, 1960) pp. 1-4.

(54) W. Shockley, Electrons and Holes in Semiconductors (D. Van Nostrand Co., Inc., New York, 1950) pp. 204-215.

(55) C. Kittel (1967), op. cit., p. 243.

(56) W. Shockley (1950), op. cit., p. 215.

(57) E. H. Putley (1960), op. cit., p. 82.

(58) W. Shockley (1950), op. cit., p. 317.

(59) E. H. Putley (1960), op. cit., p. 41.

(60) E. H. Putley (1960), op. cit., pp. 23-64.

(61) A. R. Clawson and H. H. Wieder, Solid State Electronics 7, 387 (1964).

(62) G. D. Achenbach, W. J. James, and R. Gerson, J. Am. Ceram. Soc., Vol. 50, 437 (1967).

(63) J. P. Canner, personal communication, Feb., 1968.

(64) R. T. Smith, G. D. Achenbach, R. Gerson and W. J. James, J. Appl. Phys. 39, 70 (1968).

(65) A. C. Melissinos, Experiments in Modern Physics (Academic Press Inc., New York, 1966) p. 91.

(66) J. F. Gibbons, Semiconductor Electronics (McGraw-Hill Inc., New York, 1966) p. 87.

VITA

The author was born August 31, 1942 in Cleveland, Ohio. He attended public schools in Glendale and Kirkwood, Missouri. He was graduated from Kirkwood High School in May, 1960.

He enrolled in the Missouri School of Mines and Metallurgy, Rolla, Missouri in September, 1960 in the Mechanical Engineering Department. He received a Bachelor of Science degree in Physics in 1966, after transferring into the Physics Department in 1963.

He entered the Graduate School of the University of Missouri at Rolla in 1966. He held a research assistantship from March, 1967 to January, 1968 in the Rock Mechanics and Explosive Research Group, and a research assistantship in the Physics Department from February, 1968 to July, 1968.

He is married to the former Kathleen Louise Thompson of St. Louis, Missouri and is expecting his first child in November, 1968.